82 *Inorg. Chem.* **2010**, *49*, 82–96
DOI: 10.1021/ic901405h

Inorganic Chemistry
Article

Synthesis, Characterization, and Ligand Exchange Reactivity of a Series of First Row Divalent Metal 3-Hydroxyflavonolate Complexes

Katarzyna Grubel,[†] Katarzyna Rudzka,[†] Atta M. Arif,[‡] Katie L. Klotz,[§] Jason A. Halfen,[§] and Lisa M. Berreau*[,†]

[†]*Department of Chemistry & Biochemistry, Utah State University, Logan, Utah 84322-0300,*
[‡]*Department of Chemistry, University of Utah, Salt Lake City, Utah 84112-0850, and*
[§]*Department of Chemistry, University of Wisconsin-Eau Claire, Eau Claire, Wisconsin 54702*

Received July 17, 2009

A series of divalent metal flavonolate complexes of the general formula [(6-Ph_2TPA)M(3-Hfl)]X (**1**−**5-X**; X = OTf^- or ClO_4^-; 6-Ph_2TPA = *N*,*N*-bis((6-phenyl-2-pyridyl)methyl)-*N*-((2-pyridyl)methyl)amine; M = Mn(II), Co(II), Ni(II), Cu(II), Zn(II); 3-Hfl = 3-hydroxyflavonolate) were prepared and characterized by X-ray crystallography, elemental analysis, FTIR, UV−vis, ^{1}H NMR or EPR, and cyclic voltammetry. All of the complexes have a bidentate coordinated flavonolate ligand. The difference in M−O distances (Δ_{M-O}) involving this ligand varies through the series, with the asymmetry of flavonolate coordination increasing in the order Mn(II) ∼ Ni(II) < Cu(II) < Zn(II) < Co(II). The hypsochromic shift of the absorption band I ($\pi \rightarrow \pi^*$) of the coordinated flavonolate ligand in **1**−**5-OTf** (relative to that in free anion) increases in the order Ni(II) < Mn(II) < Cu(II) < Zn(II), Co(II). Previously reported 3-Hfl complexes of divalent metals fit well with this ordering. ^{1}H NMR studies indicate that the 3-Hfl complexes of Co(II), Ni(II), and Zn(II) exhibit a pseudo-octahedral geometry in solution. EPR studies suggest that the Mn(II) complex **1-OTf** may form binuclear structures in solution. The mononuclear Cu(II) complex **4-OTf** has a distorted square pyramidal geometry. The oxidation potential of the flavonolate ligand depends on the metal ion present and/or the solution structure of the complex, with the Mn(II) complex **1-OTf** exhibiting the lowest potential, followed by the pseudo-octahedral Ni(II) and Zn(II) 3-Hfl complexes, and the distorted square pyramidal Cu(II) complex **4-OTf**. The Mn(II) complex [(6-Ph_2TPA)Mn(3-Hfl)]OTf (**1-OTf**) is unique in the series in undergoing ligand exchange reactions in the presence of $M(ClO_4)_2 \cdot 6H_2O$ (M = Co, Ni, Zn) in CD_3CN to produce $[(6\text{-}Ph_2TPA)M(CD_3CN)_n](X)_2$, $[Mn(3\text{-}Hfl)_2 \cdot 0.5H_2O]$, and MnX_2 (X = OTf^- or ClO_4^-). Under similar conditions, the 3-Hfl complexes of Co(II), Ni(II), and Cu(II) undergo flavonolate ligand exchange to produce $[(6\text{-}Ph_2TPA)M(CD_3CN)_n](X)_2$ (M = Co, Ni, Cu; *n* = 1 or 2) and $[Zn(3\text{-}Hfl)_2 \cdot 2H_2O]$. An Fe(II) complex of 3-Hfl, $[(6\text{-}Ph_2TPA)Fe(3\text{-}Hfl)]ClO_4$ (**8**), was isolated and characterized by elemental analysis, FTIR, UV−vis, ^{1}H NMR, cyclic voltammetry, and a magnetic moment measurement. This complex reacts with O_2 to produce the diiron(III) μ-oxo compound $[(6\text{-}Ph_2TPAFe(3Hfl))_2(\mu\text{-}O)](ClO_4)_2$ (**6**).

Introduction

Flavonoids are polyphenolic compounds that are produced in plants.[1] One of these compounds, quercetin (Scheme 1), is found in many fruits and vegetables, and is of considerable current interest for its antioxidant and antimicrobial properties.[2,3] In the soil environment, fungal and bacterial quercetin dioxygenases catalyze oxidative carbon−carbon bond cleavage and CO release from a metal-coordinated quercetin in a 2,4-dioxygenolytic ring cleavage reaction. Fungal quercetinases are known to contain a mononuclear Cu(II) center and have been extensively investigated.[4−9] Studies of a bacterial quercetinase from *Bacillus subtilis* (YxaG) showed that when this enzyme is produced in *Escherichia coli* it will bind a variety of divalent metals, with the highest level of reactivity being found for Mn(II).[10,11]

*To whom correspondence should be addressed. E-mail: lisa.berreau@usu.edu. Phone: (435) 797-1625. Fax: (435) 797-3390.

(1) Iwashina, T. *J. Plant Res.* **2000**, *113*, 287–299.
(2) Pietta, P.-G. *J. Nat. Prod.* **2000**, *63*, 1035–1042.
(3) Cushine, T. P. T.; Lamb, A. J. *Int. J. Antimicrob. Agents* **2005**, *26*, 343–356.
(4) Oka, T.; Simpson, F. J. *Biochem. Biophys. Res. Commun.* **1971**, *43*, 1–5.
(5) Oka, T.; Simpson, F. J.; Krishnamurty, H. G. *Can. J. Microbiol.* **1972**, *18*, 493–508.
(6) Hund, H. K.; Breuer, J.; Lingens, F.; Huttermann, J.; Kappl, R.; Fetzner, S. *Eur. J. Biochem.* **1999**, *263*, 871–878.
(7) Tranchimand, S.; Ertel, G.; Gaydou, V.; Gaudin, C.; Tron, T.; Iacazio, G. *Biochimie* **2008**, *90*, 781–789.
(8) Kooter, I. M.; Steiner, R. A.; Dijkstra, B. W.; van Noort, P. I.; Egmond, M. R.; Huber, M. *Eur. J. Biochem.* **2002**, *269*, 2971–2979.
(9) Fusetti, F.; Schroter, K. H.; Steiner, R. A.; van Noort, P. I.; Pijning, T.; Rozeboom, H. J.; Kalk, K. H.; Egmond, M. R.; Dijkstra, B. W. *Structure* **2002**, *10*, 259–268.
(10) Gopal, B.; Madan, L. L.; Betz, S. F.; Kossiakoff, A. A. *Biochemistry* **2005**, *44*, 193–201.
(11) Schaab, M. R.; Barney, B. M.; Francisco, W. A. *Biochemistry* **2006**, *45*, 1009–1016.

 Published on Web 12/02/2009

Scheme 1

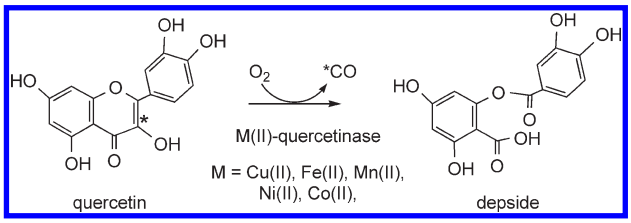

Recent investigations of a quercetinase from *Streptomyces sp*. FLA expressed in *E. coli* revealed that this enzyme is most active in the presence of Ni(II), with the next highest level of activity being found with Co(II).[12]

The quercetinase enzymes from *Aspergillus japonicus* and *B. subtilis* have been characterized by X-ray crystallography.[9,10] Both are members of the cupin superfamily of proteins (bicupins), with two well-separated active site metal centers, each having a ligand donor set composed of three histidine donors and a glutamate ligand. In the structure of the copper-containing enzyme from *A. japonicus*, the copper centers exhibit two different geometries. One is a distorted tetrahedron composed of three histidine donors and a water molecule, and in the other, a glutamate ligand (Glu73) is also coordinated in an axial position to give an overall distorted trigonal bipyramidal copper center. These geometries are present in a ~70:30 ratio. Electron paramagnetic resonance (EPR) studies of the protein are consistent with this mixture of geometries also being present in solution. In the tetrahedral geometry, Glu73 acts as a hydrogen bond acceptor for the metal-bound water molecule. Coordination of quercetin to the copper center occurs in a monodentate fashion via the deprotonated C(3)−OH moiety, with Glu73 possibly acting as the active site base for substrate deprotonation.[13] The overall geometry of the copper center in the enzyme/substrate adduct is distorted trigonal bipyramidal. A key feature of the coordinated quercetin is pyramidalization of the C(2) atom indicating increased sp^3 character that may stabilize radical formation in a reaction involving O_2.

The *B. subtilis* enzyme was initially reported to be an Fe(II)-containing quercetin 2,3-dioxygenase,[14,15] and was crystallized with Fe(II) present in both active sites of this bicupin enzyme.[10] Both metal centers exhibit a coordination number of five, with three histidine donors, a glutamate, and a water molecule. The overall geometry of the Fe(II) center is distorted trigonal bipyramidal in the *N*-terminal active site and distorted square pyramidal in the *C*-terminal domain of the protein. Metal ion replacement studies of the *B. subtilis* enzyme (via reconstitution of the apoenzyme) indicated increased levels of activity for Mn(II)- and Co(II)-containing enzyme (35- and 24-fold, respectively) relative to that found for Fe(II). On the basis of this data, it has been suggested that Mn(II) may be the preferred metal cofactor for the *B. subtilis* enzyme. EPR studies of the Mn(II)-containing enzyme from *B. subtilis* suggest octahedral coordination of the metal center.[11]

The quercetinase QueD from *Streptomyces sp. FLA* is a monocupin dioxygenase.[16] When overexpressed in *E. coli*, this enzyme exhibited the highest level of activity when Ni(II) and Co(II) salts were added to the LB medium.[12,17] An increase in activity was not observed when Mn(II), Fe(II), Cu(II), or Zn(II) was added. EPR studies of the cobalt-containing enzyme indicate a high-spin ($S = 3/2$) Co(II) center in a trigonal bipyramidal or tetrahedral geometry in the resting state. EPR experiments performed in the presence of quercetin and O_2 revealed no evidence of a change in valency of the cobalt ion during substrate turnover.[12]

Different mechanistic pathways have been proposed for the spin-forbidden, O_2-dependent quecetin oxidation reaction depending on whether a redox active metal center is present in the active site of the enzyme. For Cu(II)-containing quercentinase enzymes, it is unlikely that O_2 will coordinate to the type II oxidized metal center, and the reaction is suggested to involve valence tautomerism between the Cu(II)-quercetin adduct and a Cu(I)-flavonoxy radical species, the latter of which can act as a one-electron reductant toward O_2. The pyramidalization of the C(2) center identified in the X-ray structure of the ES adduct of the *A. japonicus* enzyme suggests possible stabilization of the radical at this atom.[13] For redox-active metal ions such as Mn(II), the metal center may serve as an electron conduit in an adduct wherein both the flavonolate and the O_2 coordinate to the metal center prior to oxygen activation. Specifically, electron transfer from the metal center to coordinated O_2, with subsequent electron transfer from the coordinated quercetin monoanion to the oxidized metal center, would generate a quercetin radical-M(II)-O_2^- species, from which C−C bond cleavage and CO release could proceed. This proposed mechanism is similar to the reaction pathway suggested for Fe(II)- and Mn(II)-containing extradiol catechol dioxygenases.[18]

Overall, from studies of the *A. japonicus*, *B. subtilis*, and *Streptomyces sp. FLA* quercetinases, possible roles for the divalent metal center in substrate oxidation have been suggested to include the following: (1) reduction of the pK_a of quercetin to enable substrate deprotonation, (2) stabilization of the flavonolate intermediate, (3) influence on the coordination mode (mono- versus bidentate) and redox potential of the bound flavonolate, (4) facilitation of the formation of radical character on the coordinated flavonolate via valence tautomerism, and (5) acting as a redox conduit for structures wherein both flavonolate and O_2 are coordinated to the metal center.

Model studies of copper-containing forms of quercetinases have demonstrated that both Cu(I) and Cu(II) flavonolate complexes undergo reaction with O_2 to produce CO and the depside.[19] Kinetic studies of the reaction involving the Cu(II) complex [Cu(3-Hfl)$_2$] (3-Hfl = 3-hydroxyflavonolate) with O_2 in DMF indicate a rate law that is second-order overall ($-d[Cu(3\text{-}Hfl)_2]/dt = k_{obs}[Cu(3\text{-}Hfl)_2][O_2]$). In the presence of pyridine, the observed rate increases by ~2.5-fold, which

(12) Merkens, H.; Kappl, R.; Jakob, R. P.; Schmid, F. X.; Fetzner, S. *Biochemistry* **2008**, *47*, 12185–12196.
(13) Steiner, R. A.; Kalk, K. H.; Dijkstra, B. W. *Proc. Natl. Acad. Sci.* **2002**, *99*, 16625–16630.
(14) Bowater, L.; Fairhurst, S. A.; Just, V. J.; Bornemann, S. *FEBS Lett.* **2004**, *557*, 45–48.
(15) Barney, B. M.; Schaab, M. R.; LoBrutto, R.; Francisco, W. A. *Protein Expression Purif.* **2004**, *35*, 131–141.
(16) Merkens, H.; Sielker, S.; Rose, K.; Fetzner, S. *Arch. Microbiol.* **2007**, *187*, 475–487.
(17) Based on comparison of k_{cat} and K_M values with those of Fe(II)-containing enzyme.
(18) Emerson, J. P.; Kovaleva, E. G.; Farquhar, E. R.; Lipscomb, J. D.; Que, L. *Proc. Natl. Acad. Sci.* **2008**, *105*, 7347–7352 and references cited therein.
(19) Kaizer, J.; Balogh-Hergovich, E.; Czaun, M.; Csay, T.; Speier, G. *Coord. Chem. Rev.* **2006**, *250*, 2222–2233.

has been attributed to a change in the coordination mode of the flavonolate ligand from bidentate to monodentate. Model studies involving other divalent metal ions are considerably fewer in number. Catalytic oxygenation of 3-hydroxyflavone derivatives by bis(salicylidene)ethylenediaminatocobalt(II) ([Co(salen]) at room temperature has been reported.[20] This catalysis occurs in the presence of DMSO and DMF, but not in methanol, THF, or CH_2Cl_2. The involvement of a $Co-O_2$ complex in the reaction has been proposed. A Co(III) complex, [Co(III)(salen)(4′MeOflaH)], was found to be susceptible to oxygenation in pyridine and DMF, but was found to be stable to oxygen in non-coordinating solvents. This O_2 reactivity correlates with dissociation of the flavonolate ligand from the Co(III) center.[21,22] Two recent studies outlined the structural and O_2 reactivity properties of Fe(III) and Mn(II) flavonolate complexes.[23,24] Fe(III)(4′MeOflaH)$_3$ and Mn(II)(3-Hfl)$_2$(py)$_2$ were found to undergo reaction with O_2 at 100 °C in DMF with second-order rate constants of 0.50 M^{-1} s^{-1} and 0.08 M^{-1} s^{-1}, respectively. On the basis of comparison of rate constants at 100 °C, these complexes are more reactive than the copper analogues Cu(3-Hfl)$_2$ (k = 0.0087 M^{-1} s^{-1}) and Cu(3-Hfl)$_2$(py)$_2$ (0.04 M^{-1} s^{-1}), suggesting a metal dependent reactivity order of Fe(III) > Mn(II) > Cu(II).[23] The Fe(III) complex Fe(III)(salen)(3-Hfl) contains a bidentate flavonolate ligand and undergoes reaction with O_2 at elevated temperatures (100−120 °C).[24] In the presence of excess carboxylate anion, the rate of reaction with O_2 increases, with bulky carboxylates (e.g., triphenyl acetate) producing the greatest rate enhancement (~2 orders of magnitude at 100 °C). This is attributed to the formation of a more reactive monondentate flavonolatoiron(III) complex. Evidence for direct electron transfer from the flavonolate ligand to O_2 to form O_2^- was found in the reaction via the use of the superoxide scavenger nitroblue tetrazolium (NBT).

From the studies described above and investigations of the O_2 reactivity of non-coordinated flavonolate anions, it is clear that enhancing the electron density within the flavonolate anion through deprotonation and limiting its coordination mode to monodentate are key factors in enhancing the rate of oxygenation. What is currently unclear is how differences in the divalent metal ion present in quercetinase enzymes produce differing rates of oxygenation, as has been found for the *B. subtilis* and *Streptomyces sp. FLA* enzymes. Such differences may result from modulation of the coordination mode and/or the redox potential of the flavonolate, or may relate to the ability of the metal center to serve as a redox conduit. As an approach toward systematically examining the influence of the divalent metal ion, we report the preparation and characterization of the first extensive series of structurally related divalent metal flavonolate complexes. Our initial goal in this research was to examine how differences in the divalent metal center (Mn(II), Fe(II), Co(II), Ni(II), Cu(II), and Zn(II)) influence flavonolate coordination, and spectroscopic and redox properties. The choice of the tetradentate 6-Ph$_2$TPA ligand as the supporting scaffold was based on its relevance to the coordination environment in enzymes of the cupin superfamily.[25] We have previously used this ligand to study chemistry of relevance to Ni(II)-acireductone dioxygenase,[26−29] another dioxygenase of the cupin superfamily that produces CO upon substrate oxygenation. The results presented herein indicate that the nature of the divalent metal ion influences the coordination mode and redox potential of a 3-Hfl ligand in complexes of the general formula [(6-Ph$_2$TPA)M(3-Hfl)]X (M=Mn(II), Co(II), Ni(II), Cu(II), Zn(II); X = OTf^- or ClO_4^-). In the course of characterizing the Mn(II) complex, we found evidence for ligand exchange reactions, which were subsequently further explored. The Fe(II) flavonolate complex [(6-Ph$_2$TPA)Fe(3-Hfl)]ClO_4 was prepared and characterized, albeit an X-ray structure was not obtained. This is because the complex is very O_2 sensitive and quickly undergoes reaction to produce a diiron(III) μ-oxo compound, wherein each iron center has a coordinated flavonolate ligand. The structure of this diiron(III) complex was determined by X-ray crystallography.

Experimental Section

General and Physical Methods. All chemicals were purchased from commercial sources and used as received unless otherwise noted. Synthetic reactions were performed in a MBraun Unilab glovebox under a N_2 atmosphere. Solvents for glovebox use were dried according to published methods and distilled under N_2 prior to use.[30] The 6-Ph$_2$TPA ligand was prepared as previously described.[25]

^{1}H NMR spectra of **2**−**5** were obtained in CD_3CN solution on a Bruker ARX-400 spectrometer. Data was collected for paramagnetic complexes as previously described.[26] Chemical shifts (in ppm) are referenced to the residual solvent peak(s) in CHD_2CN (^{1}H, 1.94 (quintet) ppm). FTIR spectra were collected using KBr pellets on a Shimadzu FTIR-8400 spectrometer. UV−vis spectra were recorded at ambient temperature using a Hewlett-Packard 8453 diode array spectrophotometer. Cyclic voltammetry data was collected using a BAS-Epsilon system.[25] Conditions for the CV experiments are listed in a footnote of Table 3 and in the text. EPR spectra were collected on a Bruker EMX-Plus spectrometer fitted with a liquid helium cooled probe. ESI/APCI and MALDI mass spectral data for complexes was collected at the Mass Spectrometry Facility, University of California, Riverside. Room temperature magnetic susceptibilities were determined by the Evans method.[31] Elemental analyses were performed by Atlantic Microlab, Inc., Norcross, GA.

Caution! *Perchlorate salts of metal complexes with organic ligands are potentially explosive. Only small amounts of material should be prepared, and these should be handled with great care.*[32]

General Procedure for the Synthesis of [(6-Ph$_2$TPA)M(3-Hfl)]OTf Complexes. (a)M = Mn (1-OTf), Cu (4-OTf), or Zn (5-OTf). In a N_2-filled glovebox, a methanol solution (2 mL)

(20) Nishinaga, A.; Tojo, T.; Matsuura, T. *J. Chem. Soc., Chem. Commun.* **1974**, 896–897.
(21) Nishinaga, A.; Numada, N.; Maruyama, K. *Tetrahedron Lett.* **1989**, *30*, 2257–2258.
(22) Nishinaga, A.; Kuwashige, T.; Tsutsui, T.; Mashino, T.; Maruyama, K. *J. Chem. Soc., Dalton Trans.* **1994**, 805–810.
(23) Kaizer, J.; Baráth, G.; Pap, J.; Speier, G.; Giorgi, M.; Réglier, M. *Chem. Commun.* **2007**, 5235–5237.
(24) Baráth, G.; Kaizer, J.; Speier, G.; Párkányi, L.; Kuzmann, E.; Vértes, A. *Chem. Commun.* **2009**, 3630–3632.
(25) Makowska-Grzyska, M. M.; Szajna, E.; Shipley, C.; Arif, A. M.; Mitchell, M. H.; Halfen, J. A.; Berreau, L. M. *Inorg. Chem.* **2003**, *42*, 7472–7488.
(26) Szajna, E.; Dobrowolski, P.; Fuller, A. L.; Arif, A. M.; Berreau, L. M. *Inorg. Chem.* **2004**, *43*, 3988–3997.
(27) Szajna, E.; Arif, A. M.; Berreau, L. M. *J. Am. Chem. Soc.* **2005**, *127*, 17186–17187.
(28) Szajna-Fuller, E.; Rudzka, K.; Arif, A. M.; Berreau, L. M. *Inorg. Chem.* **2007**, *46*, 5499–5507.
(29) Szajna-Fuller, E.; Chambers, B. M.; Arif, A. M.; Berreau, L. M. *Inorg. Chem.* **2007**, *46*, 5486–5498.
(30) Armarego, W. L. F.; Perrin, D. D. *Purification of Laboratory Chemicals*, 4th ed.; Butterworth-Heinemann: Boston, MA, 1996.
(31) Evans, D. F. *J. Chem. Soc.* **1959**, 2003–2005.
(32) Wolsey, W. C. *J. Chem. Educ.* **1973**, *50*, A335–A337.

of $M(OTf)_2$ (1.37×10^{-4} mol) was added to solid 6-Ph_2TPA (1.37×10^{-4} mol), and the mixture was stirred until all of the chelate ligand had dissolved. The resulting solution was added to a methanol solution (2 mL) containing 3-Hfl (1.37×10^{-4} mol) and $Me_4NOH \cdot 5H_2O$ (1.37×10^{-4} mol). The mixture was then allowed to stir overnight at ambient temperature. The reaction mixture was taken out of the glovebox, and the solvent was removed under reduced pressure. The residual solid was suspended on the top of a Celite plug and washed several times with distilled water. The wet solid was then dissolved in CH_2Cl_2, and the filtrate was collected and brought to dryness under reduced pressure. The residue was dissolved in CH_2Cl_2, and the analytically pure microcrystalline flavonolate complex was precipitated via the addition of excess Et_2O and cooling of the mixture at −30 °C for 12 h.

Note Regarding Experimental Data. Extensive characterization data (FTIR, UV−vis, mass spectrometry, magnetic moment, cyclic voltammetry) for the triflate compounds **1**−**5-OTf** is provided in Table 3. Selected data for the perchlorate analogues **1**−**5-ClO$_4$**, which were primarily prepared for X-ray crystallographic studies, is given below.

[(6-Ph$_2$TPA)Mn(3-Hfl)]OTf (1-OTf). Yield: 73% (green crystals).

[(6-Ph$_2$TPA)Cu(3-Hfl)]OTf (4-OTf). Yield: 74% (dark green crystals).

[(6-Ph$_2$TPA)Zn(3-Hfl)]OTf (5-OTf). Yield: 98% (yellow crystals). ^{1}H NMR (CD_3CN, 400 MHz): δ 8.53 (d, J = 5.2 Hz, 1 H), 8.18 (dt, J = 7.3 Hz, J = 1.5 Hz, 2 H), 7.92 (td, J = 7.8 Hz, J = 1.7 Hz, 1 H), 7.78 (t, J = 7.7 Hz, 2 H), 7.65 (m, 3 H), 7.39 (m, 11 H), 7.13 (dt, J = 6.8 Hz, J = 1.5 Hz, 4 H), 7.03 (tt, J = 7.4 Hz, J = 1.2 Hz, 2 H), 6.94 (tt, J = 8.0 Hz, J = 1.5 Hz, 4 H), 4.85 (d, J = 14.7 Hz, 2 H), 4.51 (d, J = 14.8 Hz, 2 H), 4.39 (s, 2 H); ^{13}C{^{1}H} NMR (CD_3CN, 400 MHz): δ 187.7, 168.1, 164.0, 163.8, 162.9, 156.5, 154.6, 148.8, 147.6, 146.3, 141.1, 140.5, 137.4, 136.8, 136.1, 135.7, 135.6, 135.1, 134.8, 132.2, 131.9, 131.3, 130.9, 130.2, 130.1, 125.8, 125.2, 64.9, 61.5 (29 signals expected for equivalent phenyl-appended pyridyl donors; 29 observed).

(b)M = Co (2-OTf) or Ni (3-OTf). Under a nitrogen atmosphere, a methanol (∼2 mL) solution of $MCl_2 \cdot 5H_2O$ (1.37×10^{-4} mol) was added to solid 6-Ph_2TPA (1.37×10^{-4} mol), and the mixture was stirred until all of the chelate ligand had dissolved. Two equivalents of silver triflate (AgOTf; 2.74×10^{-4} mol) was then added to the mixture. After stirring for 30 min, the solution was filtered through a Celite/glass wool plug. The filtrate was added to a methanol solution (∼2 mL) containing 3-Hfl (1.37×10^{-4} mol) and $Me_4NOH \cdot 5H_2O$ (1.37×10^{-4} mol). The resulting solution was stirred overnight at ambient temperature. At this time, the reaction was taken out of the glovebox, and the solvent was removed under reduced pressure. Using a workup procedure identical to that described above for **1-OTf**, analytically pure microcrystalline products were obtained.

[(6-Ph$_2$TPA)Co(3-Hfl)]OTf (2-OTf). Yield: 54% (dark red crystals).

[(6-Ph$_2$TPA)Ni(3-Hfl)]OTf·0.25CH$_2$Cl$_2$ (3-OTf). Yield: 82% (green crystals). The presence of dichloromethane in the elemental analysis sample was confirmed using ^{1}H NMR spectroscopy.

General Procedure for the Synthesis of [(6-Ph$_2$TPA)M(3-Hfl)]ClO$_4$ Complexes (1−5-ClO$_4$). In a glovebox, an acetontrile solution (∼2 mL) of $M(ClO_4)_2 \cdot 6H_2O$ (M = Mn, Co, Ni, Cu, Zn; 1.37×10^{-4} mol) was added to solid 6-Ph_2TPA (1.37×10^{-4} mol), and the resulting mixture was stirred until all of the chelate ligand had dissolved. An acetonitrile slurry (∼2 mL) of tetramethylammonium hydroxide pentahydrate ($Me_4NOH \cdot 5H_2O$; 1.37×10^{-4} mol) and 3-hydroxyflavone (3-Hfl; 1.37×10^{-4} mol) was then added, and the resulting mixture was stirred overnight at ambient temperature. After removal of the solvent under reduced pressure, the remaining solid was dissolved in CH_2Cl_2, and the solution was filtered through a glass wool/Celite plug. The filtrate was then brought to dryness under reduced pressure. Crystals suitable for single crystal X-ray crystallography were obtained using the following approaches at ambient temperature: **1-ClO$_4$** (green crystals), diethyl ether diffusion into a dichloromethane solution; **2-ClO$_4$** (dark red crystals) and **3-ClO$_4$** (green crystals), diethyl ether diffusion into a acetonitrile solution; and **4-ClO$_4$** (green crystals), diethyl ether diffusion into dichloromethane:isopropanol/methanol (1:0.1:1) solution. For **5-ClO$_4$**, yellow crystals were obtained from dichloromethane/diethyl ether solution at 4 °C.

The ^{1}H NMR features of **2-ClO$_4$**, **3-ClO$_4$**, and **5-ClO$_4$** match those found for the triflate analogues. **1-ClO$_4$**: Anal. Calcd for $C_{45}H_{35}ClMnN_4O_7 \cdot 1/4CH_2Cl_2$: C, 63.54; H, 4.18; N, 6.55. Found: C, 63.47; H, 4.11; N, 6.45. **2-ClO$_4$**: Anal. Calcd for $C_{45}H_{35}ClCoN_4O_7 \cdot 1/7CH_2Cl_2$: C, 63.77; H, 4.18; N, 6.59. Found: C, 64.03; H, 4.19; N, 6.54. **3-ClO$_4$**: Anal. Calcd for $C_{45}H_{35}ClN_4NiO_7$: C, 64.50; H, 4.21; N, 6.69. Found: C, 64.18; H, 3.92; N, 6.55. **4-ClO$_4$**: Anal. Calcd for $C_{45}H_{35}ClCuN_4O_7 \cdot 1/5CH_2Cl_2$: C, 63.14; H, 4.15; N, 6.52. Found: C, 63.45; H, 4.30; N, 6.31. **5-ClO$_4$**: Anal. Calcd for $C_{45}H_{35}ClN_4O_7Zn \cdot 1/5CH_2Cl_2$: C, 63.01; H, 4.14; N, 6.50. Found: C, 63.15; H, 4.31; N, 6.33.

Ligand Exchange Reactions. (a). To a solution of [(6-Ph_2TPA)Mn(3-Hfl)]OTf (9.0×10^{-6} mol) in CD_3CN (0.8 mL) solid $M(ClO_4)_2 \cdot 6H_2O$ (M = Co, Ni, or Zn; 9.0×10^{-6} mol) was added. Each reaction mixture was then capped, shaken vigorously, and a ^{1}H NMR spectrum was recorded within 15 min. For each metal perchlorate salt, the NMR spectrum is consistent with the formation of $[(6\text{-}Ph_2TPA)M(CD_3CN)_n](ClO_4)_2$ (M = Co (n = 1), Ni (n = 2), or Zn (n = 1)). The product $[Mn(3\text{-}Hfl)_2 \cdot 0.5H_2O]$ is formed in each reaction, and was isolated from the Ni(II)-containing reaction mixture and characterized by elemental analysis, FTIR, and UV−vis.

(b). In a NMR tube, a CD_3CN solution (0.8 mL) of [(6-Ph_2TPA)M(3-Hfl)]OTf (M = Co, Ni, and Cu; **2**−**4-OTf**; 7.7×10^{-6} mol) was treated with solid 0.5 equiv of $Zn(ClO_4)_2 \cdot 6H_2O$ (3.9×10^{-6} mol). Each reaction mixture was then capped, shaken vigorously, and a ^{1}H NMR spectrum was recorded within 15 min. For the reactions involving the Co(II) and Ni(II) derivatives, the ^{1}H NMR spectroscopic features are consistent with the formation of $[(6\text{-}Ph_2TPA)M(CD_3CN)_n](X)_2$ (M = Ni, n = 2; M = Co, n = 1; X = OTf^- or ClO_4^-). A poorly soluble, yellow precipitate is also formed in each reaction mixture. Spectroscopic analysis (^{1}H NMR (CD_3OD) and FTIR (KBr)) of this solid suggested the formation of $[Zn(3\text{-}Hfl)_2]$. This compound was independently synthesized via treatment of $Zn(ClO_4)_2 \cdot 6H_2O$ with 2 equiv each of 3-Hfl and $Me_4NOH \cdot 5H_2O$ in methanol, which yielded a yellow precipitate. Analysis of this material by ^{1}H NMR (CD_3OD), UV−vis, and elemental analysis indicated the formulation $[Zn(3\text{-}Hfl)_2 \cdot 2H_2O]$. The UV−vis and ^{1}H NMR spectroscopic features of this material match that of the yellow precipitate generated in the ligand exchange reaction.

Synthesis of [(6-Ph$_2$TPA)Fe(3-Hfl)]ClO$_4$ (7). Under a nitrogen atmosphere, a methanol solution (∼2 mL) of $Fe(ClO_4)_2 \cdot 6H_2O$ (1.37×10^{-4} mol) was added to solid 6-Ph_2TPA (1.37×10^{-4} mol), and the resulting mixture was stirred for 2 h at ambient temperature. The solvent was then removed under reduced pressure, and the solid was dissolved in a small amount of methanol (∼1 mL). Addition of Et_2O produced a yellow precipitate, which was dried under vacuum. A ^{1}H NMR spectrum of the complex in CD_3CN was obtained. This spectrum matched that of $[(6\text{-}Ph_2TPA)Fe(CH_3CN)](ClO_4)_2$, which has been independently generated and characterized (see Supporting Information). A methanol solution (∼2 mL) of $[(6\text{-}Ph_2TPA)Fe(CH_3CN)](ClO_4)_2$ (1.37×10^{-4} mol) was treated with 3-Hfl (1.37×10^{-4} mol) and $Me_4NOH \cdot 5H_2O$ (1.37×10^{-4} mol) dissolved in methanol (∼2 mL). The resulting mixture was stirred for 15 min, and the solvent was then removed under

vacuum. The remaining green-yellow solid was dissolved CH_2Cl_2 (~2 mL) and passed through a Celite/glass wool plug. The filtrate was brought to dryness under reduced pressure, and the resulting solid (yield: 96%) was analyzed by ^{1}H NMR, FTIR, UV−vis, a magnetic moment measurement, and elemental analysis. FTIR (KBr, cm^{-1}) 1558 ($\nu_{C=O}$); UV−vis (CH_3CN) nm (ε, M^{-1} cm^{-1}) 415 (14700); μ_{eff} = 4.7 μB. Anal. Calcd for $C_{45}H_{35}ClFeN_4O_7$: C, 64.72; H, 4.22; N, 6.71. Found: C, 65.23; H, 4.28; N, 6.71.

Reactivity of [(6-Ph$_2$TPA)Fe(3-Hfl)]ClO$_4$ in Air; Isolation of [(6-Ph$_2$TPAFe(3-Hfl))$_2$(μ-O)](ClO$_4$)$_2$ (6). A methanol solution (~2 mL) of [(6-Ph$_2$TPA)Fe(3-Hfl)]ClO_4 was prepared by mixing equimolar amounts (1.37×10^{-4} mol) of 6-Ph$_2$TPA, Fe$(ClO_4)_2 \cdot 6H_2O$, $Me_4NOH \cdot 5H_2O$ and 3-Hfl and stirring under a nitrogen atmosphere for 2 h. The solvent was then removed under reduced pressure and the remaining solid was dissolved in CH_2Cl_2 (~2 mL) and filtered through a Celite/glass wool plug. The filtrate was then brought to dryness. A portion of the solid (8.45×10^{-5} mol) was dissolved in CH_3CN (~ 5 mL) and this solution was exposed to air for 24 h. Diethyl ether was then diffused into the CH_3CN solution, resulting in the deposition of dark-brown crystals suitable for single crystal X-ray crystallography. Yield: 58%. UV−vis (MeOH), nm (ε, M^{-1} cm^{-1}) 388 (24400), 490 (7300); ESI/APCI-MS, m/z (relative intensity) 743.2 ($[M - 2ClO_4]^{2+}$, 69%). Anal. Calcd for: $C_{90}H_{70}Cl_2Fe_2N_8O_{15} \cdot 2H_2O$: C, 62.77; H, 4.33; N, 6.51. Found: C, 62.96; H, 4.19; N, 6.70.

X-ray Crystallography. For each compound, **1−5-ClO$_4$** and **6**, a single crystal was mounted on a glass fiber with traces of viscous oil and then transferred to a Nonius KappaCCD diffractometer equipped with Mo Kα radiation (λ = 0.71073 Å) for data collection. For unit cell determination, 10 frames of data were collected at 150(1) K with an oscillation range of 1 deg/frame and an exposure time of 20 s/frame. Final cell constants were determined from a set of strong reflections from the actual data collection. Reflections were indexed, integrated, and corrected for Lorentz, polarization, and absorption effects using DENZO-SMN and SCALEPAC.[33] The structures were solved by a combination of direct and heavy-atom methods using SIR 97.[34] All of the non-hydrogen atoms were refined with anisotropic displacement coefficients. Unless otherwise stated, all hydrogen atoms were assigned isotropic displacement coefficients $U(H) = 1.2U(C)$ or $1.5U(C_{methyl})$, and their coordinates were allowed to ride on their respective carbons using SHELXL97.[35]

Structure Solution and Refinement. Complex **1-ClO$_4$** crystallizes in the space group $P2_1/n$, with a disordered ClO_4^- in the asymmetric unit. Complex **2-ClO$_4$** crystallizes in the space group $C2/c$ with two cation/anion pairs per asymmetric unit along with two molecules of CH_3CN. The differences in the cations (with the second being labeled with (A)) are subtle, with the most noticeable differences being in one Co−N_{PhPy} bond distance and in O−Co−N bond angles involving the O(1) atom of the flavonolate and nitrogen atoms of the chelate ligand. One of the two CH_3CN solvate molecules is composed of two 50% occupied positions for all heavy atoms. Complex **3-ClO$_4$** crystallizes in the space group $P2_1/a$. Two oxygen atoms of the perchlorate anion exhibit disorder (80:20) over two positions. Complex **4-ClO$_4$** crystallizes in the space group $P2_1/c$. One molecule of diethyl ether is also present in the asymmetric unit. Complex **5-ClO$_4$** crystallizes in the space group $P\bar{1}$. Two independent cation/anion pairs and two CH_2Cl_2 solvent molecules are found in the asymmetric unit. The two cations (with the second being labeled with (A)) have very minor differences in bond lengths/angles involving the Zn(II) center, and both exhibit a distorted square pyramidal geometry (τ = 0.35).[36] One CH_2Cl_2 solvate exhibits disorder over two positions (50:50) for each heavy atom. Complex **6** crystallizes in the space group $P\bar{1}$ with $2.5CH_3CN$ solvate molecules per asymmetric unit. Two oxygen atoms and the chlorine atom of a perchlorate anion are disordered over two positions (90:10).

Results

The goal of this investigation was to prepare and comprehensively characterize a structurally similar set of divalent metal flavonolate complexes as a prelude to O_2 reactivity studies of these complexes. The metal ions employed are those of relevance to bacterial and fungal quercetin dioxygenases (Mn(II), Fe(II), Co(II), Ni(II), Cu(II)). For spectroscopic and redox behavior comparisons, the d^{10} Zn(II) flavonolate analogue complex was also prepared.

Synthesis. Divalent metal flavonolate complexes of the general formula [(6-Ph$_2$TPA)M(3-Hfl)]X were prepared by the synthetic routes outlined in Scheme 2. Triflate derivatives were isolated as analytically pure polycrystalline materials. Perchlorate analogues were found to be highly crystalline materials suitable for single crystal X-ray crystallography. All syntheses were performed under a N_2 atmosphere.

X-ray Crystallography. The perchlorate analogues **1−5-ClO$_4$** were characterized by single crystal X-ray crystallography. A summary of the data acquisition and refinement parameters are given in Table 1. Selected bond distances and angles are given in Table 2 and Supporting Information, Table S1, respectively.

Thermal ellipsoid drawings of the Mn(II) (**1-ClO$_4$**) and Ni(II) (**3-ClO$_4$**) complexes are shown in Figure 1. Each metal center exhibits a pseudo-octahedral geometry with the ketone oxygen (O(2)) of the flavonolate positioned *trans* to the tertiary amine nitrogen of the chelate ligand. In both complexes, the flavonolate ligand is located between the two hydrophobic phenyl appendages of the chelate ligand.

To our knowledge, complex **1-ClO$_4$** is the first Mn(II) complex of the 6-Ph$_2$TPA ligand to exhibit coordination of both phenyl-appended pyridyl donors. Complexes having an additional bidentate ligand, such as the hydroxamate complex $[(\kappa^3\text{-6-Ph}_2\text{TPAMn})_2(\mu\text{-ONHC(O)CH}_3)_2](ClO_4)_2$[25] and the oxalate derivative $[(\kappa^3\text{-6-Ph}_2\text{TPAMn})_2(\mu\text{-C}_2\text{O}_4)](ClO_4)_2$,[37] have previously been found to exhibit κ^3-coordination (facial and meridional, respectively) of the chelate ligand, with one non-coordinated phenylpyridyl appendage. In **1-ClO$_4$**, the Mn(1)−O(1) and Mn(1)−O(2) distances (2.121(3) Å and 2.143(3) Å, respectively) are similar. In the only other Mn(II) complex of 3-Hfl reported to date, $[(Mn(3\text{-Hfl})_2(py)_2]$,[23] the Mn−O distances differ by ~0.06 Å, with the bond involving the ketone oxygen being longer. The average Mn−O distance in **1-ClO$_4$** (2.13 Å) is shorter than that found in $[(Mn(3\text{-Hfl})_2(py)_2]$ (2.16 Å).[23] The average Mn−N distance in **1-ClO$_4$** is ~2.33 Å, which is similar to that found in $[(\kappa^3\text{-6-Ph}_2\text{TPAMn})_2(\mu\text{-ONHC(O)CH}_3)_2](ClO_4)_2$[25] and $[(\kappa^3\text{-6-Ph}_2\text{TPAMn})_2(\mu\text{-C}_2\text{O}_4)](ClO_4)_2$.[37]

(33) Otwinowski, Z.; Minor, W. *Methods Enzymol*. **1997**, *276*, 307–326.
(34) Altomare, A.; Burla, M. C.; Camalli, M.; Cascarano, G. L.; Giacovazzo, C.; Guagliardi, A.; Moliterni, A. G. G.; Polidori, G.; Spagna, R. *J. Appl. Crystallogr*. **1999**, *32*, 115–119.
(35) Sheldrick, G. M. *SHELXL97*; University of Göttingen: Göttingen, Germany, 1997.
(36) Addison, A. W.; Rao, T. N.; Reedijk, J.; van Rijn, J.; Verschoor, G. C. *J. Chem. Soc., Dalton Trans*. **1984**, 1349–1356.
(37) Fuller, A. L.; Arif, A. M.; Berreau, L. M. unpublished result.

Scheme 2

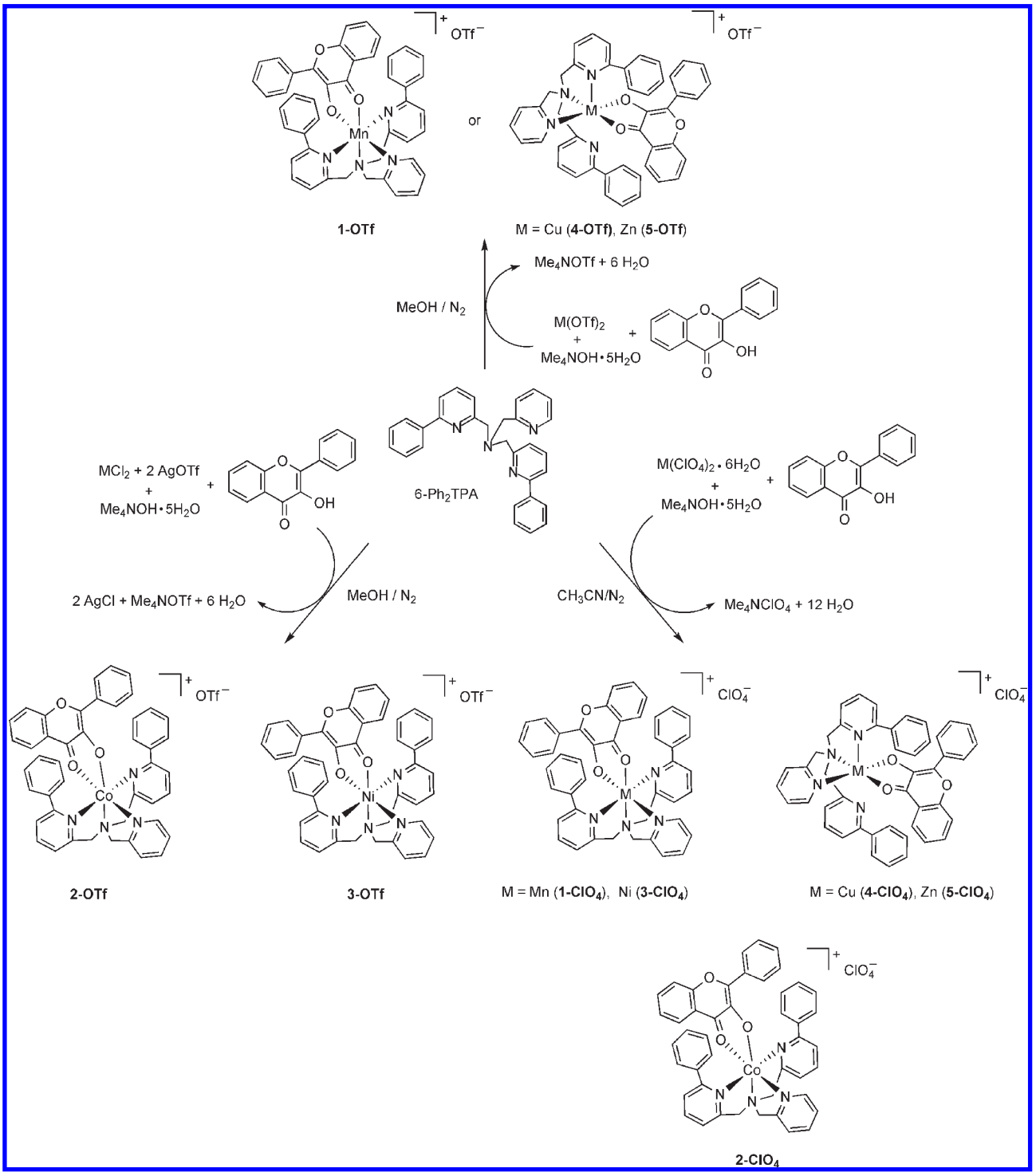

The mononuclear **3-ClO$_4$** is structurally similar to Ni(II) acetohydroxamate and enolate complexes of the 6-Ph$_2$TPA ligand.[25,28] For example, the average Ni−O and Ni−N$_{PhPy}$, as well as the N$_{Py}$ and N$_{Amine}$ distances (Table 2) are similar in these complexes. The Ni(1)−O(1) distance (1.996(2) Å) is slightly shorter than the distance involving the ketone oxygen atom (Ni(1)−O(2), 2.010(3) Å). In the only other Ni complex of 3-Hfl reported to date, [(Ni(3-Hfl)$_2$(py)$_2$],[38] the Ni−O distances are slightly longer (2.023(2) and 2.067(2) Å).

The structure of the Co(II) complex [(6-Ph$_2$TPA)Co(3-Hfl)]ClO$_4$ (**2-ClO$_4$·2CH$_3$CN**) contains two independent cation/anion pairs per asymmetric unit (the second labeled with an "A" designation). The two cations are structurally similar, each having a pseudo-octahedral geometry (Figure 2). Unlike the Mn(II) and Ni(II) analogues (**1-ClO$_4$** and **3-ClO$_4$**), this complex has the deprotonated oxygen atom of the 3-Hfl ligand positioned *trans* to the tertiary amine nitrogen atom of the chelate ligand and

(38) Farina, Y.; Yamin, B. M.; Fun, H.-K.; Yip, B.-C.; Teoh, S.-G. *Acta Crystallogr.* **1995**, *C51*, 1537–1540.

Table 1. Summary of X-ray Data Collection and Refinement[a]

	1-ClO_4	2-$ClO_4 \cdot 2CH_3CN$	3-ClO_4	4-$ClO_4 \cdot Et_2O$	5-$ClO_4 \cdot 2CH_2Cl_2$
empirical formula	$C_{45}H_{35}ClMnN_4O_7$	$C_{94}H_{76}Cl_2Co_2N_{10}O_{14}$	$C_{45}H_{35}ClN_4NiO_7$	$C_{49}H_{45}ClCuN_4O_8$	$C_{92}H_{74}Cl_6N_8O_{14}Zn_2$
M_r	834.16	1758.41	837.93	916.88	1859.04
crystal system	monoclinic	monoclinic	monoclinic	monoclinic	triclinic
space group	$P2_1/n$	$C2/c$	$P2_1/a$	$P2_1/c$	$P\bar{1}$
a /Å	11.6175(8)	43.8551(6)	18.5881(4)	17.7565(6)	11.6633(2)
b /Å	16.3708(14)	18.2721(2)	19.6427(4)	12.6011(2)	18.3461(3)
c /Å	20.6689(11)	21.2336(3)	10.4897(2)	19.0305(6)	20.3958(3)
α /deg	90	90	90	90	103.0861(8)
β /deg	94.219(5)	101.7509(8)	90.4537(11)	90.0709(12)	90.5675(9)
γ /deg	90	90	90	90	98.3257(9)
V /Å^3	3920.3(5)	16658.4(4)	3829.88(13)	4258.1(2)	4201.95(12)
Z	4	8	4	4	2
D_c/Mg m^{-3}	1.413	1.402	1.453	1.430	1.469
T /K	150(1)	150(1)	150(1)	150(1)	150(1)
color	yellow	brown	yellow/green	green	yellow
crystal habit	prism	plate	dichroic prism	prism	prism
crystal size/ mm	0.38 × 0.13 × 0.13	0.38 × 0.38 × 0.20	0.35 × 0.18 × 0.10	0.25 × 0.23 × 0.05	0.28 × 0.28 × 0.15
diffractometer	Nonius KappaCCD	Nonius KappaCCD	Nonius KappaCCD	Nonius KappaCCD	Nonius KappaCCD
μ/ (mm^{-1})	0.464	0.536	0.636	0.638	0.833
$2\theta_{max}$ /deg	50.02	54.96	54.98	50.74	52
completeness to θ (%)	97.8	99.9	99.2	98.8	99.2
reflections collected	10543	36402	15907	14181	30941
independent reflections	6770	19074	8729	7731	16397
R_{int}	0.0623	0.0519	0.0410	0.0377	0.0519
variable parameters	552	1084	532	568	1127
$R1/wR2$[b]	0.0640/0.1367	0.0562/0.1411	0.0576/0.1087	0.0646/0.1564	0.0458/0.1011
goodness-of-fit (F^2)	1.043	1.027	1.036	1.029	1.027
$\Delta\rho_{max/min}$/e Å^{-3}	0.415/−0.304	1.181/−0.760	0.744/−0.672	1.093/−0.772	0.709/−0.726

[a] Radiation used: Mo Kα (λ = 0.71073 Å). [b] $R1 = \sum||F_o| - |F_c||/\sum|F_o|$; $wR2 = [\sum w(F_o^2 - F_c^2)^2/\sum w(F_o^2)^2]^{1/2}$, where $w = 1/[\sigma^2(F_o^2) + (aP)^2 + bP]$.

Table 2. Selected Bond Distances (Å) for Complexes **1**−**5-ClO_4**

	1-ClO_4	2-$ClO_4 \cdot 2CH_3CN$[a]	3-ClO_4	4-$ClO_4 \cdot Et_2O$	5-$ClO_4 \cdot 2CH_2Cl_2$[a]
M−N(1)	2.284(4)	2.111(3)	2.061(2)	1.993(3)	2.085(2)
M−N(2)	2.340(3)	2.175(2)	2.067(3)	2.029(3)	2.144(2)
M−N(3)	2.390(3)	2.244(2)	2.278(2)	2.340(3)	2.107(2)
M−N(4)	2.338(3)	2.331(3)	2.231(2)		
M−O(1)	2.121(3)	1.956(2)	1.996(2)	1.921(3)	1.951(2)
M−O(2)	2.143(3)	2.172(2)	2.031(2)	2.010(3)	2.1175(19)
Δ_{M-O}	0.022	0.22	0.035	0.089	0.17
C(31)−O(1)	1.313(4)	1.317(4)	1.315(3)	1.349(5)	1.315(3)
C(32)−O(2)	1.262(5)	1.260(4)	1.267(3)	1.252(5)	1.255(3)

[a] Data for one of two cations present in the asymmetric unit.

Table 3. Analytical, Spectroscopic, Magnetic, and Cyclic Voltammetry Data for **1**−**5-OTf**

complex	1-OTf	2-OTf	3-OTf·0.25CH_2Cl_2	4-OTf	5-OTf
Anal. Calcd. (found):					
C:	62.51 (62.05)	62.23 (61.94)	61.11 (61.06)	61.91 (62.02)	61.78 (61.74)
H:	3.99 (4.06)	3.97 (3.89)	3.97 (4.04)	3.95 (3.98)	3.94 (4.01)
N:	6.34 (6.16)	6.31 (6.11)	6.16 (5.86)	6.28 (6.21)	6.28 (6.30)
UV−vis, nm (ε, M^{-1} cm^{-1})[a]	431 (17600)	422 (17100)	443 (20000)	428 (22200)	420 (20100)
ESI-MS m/z (rel intensity) [M−OTf]$^+$	734.2059 (100)[b]	738.2037 (16)	737.2064 (15)	742.2002 (16)	743.1984 (2)
FTIR[c], cm^{-1} $\nu_{C=O}$	1550	1557	1548	1542	1552
μ_{eff}, μ_B[d]	5.90	4.38	3.34	1.93	*e*
Ep_a[f] versus Fc/Fc$^+$	+365	*g*	+506	+660[h]	+534

[a] Spectra collected in dry CH_3CN. [b] Obtaind by MALDI. [c] Spectra collected as dilute KBr pellets. [d] Determined by Evans method (Evans, D. F. *J. Chem. Soc.* **1959**, 2003). [e] Diamagnetic. [f] All cyclic voltammetry data was obtained under argon in CH_2Cl_2 with a complex concentration of 1 mM and Bu_4NClO_4 (0.1 M) as the supporting electrolyte. The scan rate was 50−100 mV/s. The experimental setup consisted of a platinum button working electrode, a silver wire reference electrode, and a platinum wire auxiliary electrode. All potentials are reported relative to an internal Fc/Fc$^+$ standard. Under these conditions, the Fc/Fc$^+$ couple is at +460 mV versus silver wire. [g] No electrochemical behavior between +1.4 V and −1.0 V. [h] A quasi-reversible reduction peak at −1088 mV vs Fc/Fc$^+$ has been tentatively assigned to the Cu(II)/Cu(I) couple as no other compound of the group has waves at potentials lower than Fc/Fc$^+$.

exhibits notably different Co−O distances (Co(1)−O(1) 1.956(2) Å; Co(1)−O(2), 2.172(2) Å). This is similar to the bidentate ligand coordination present in the Co(II) acetohydroxamate complex [(6-Ph_2TPA)Co(ONHC(O)CH_3)]-ClO_4, which exhibits Co−O bond lengths of 1.935(2) and 2.142(2) Å.[25] The average Co−N_{PhPy} distance is notably

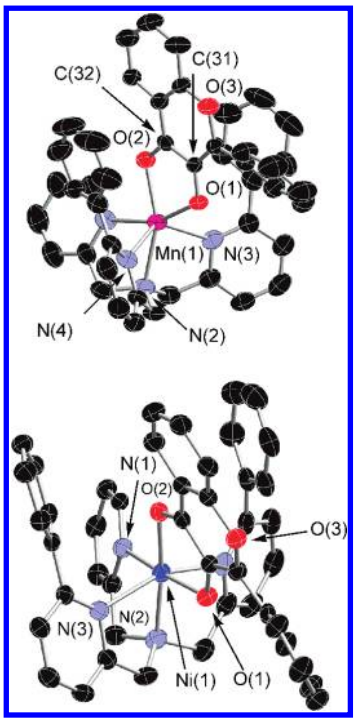

Figure 1. Thermal ellipsoid drawings (50% probability) of the cationic portions of **1-ClO$_4$** (top) and **3-ClO$_4$** (bottom). Hydrogen atoms have been omitted for clarity.

longer in **2-ClO$_4$·2CH$_3$CN** (av 2.39 Å) versus the hydroxamate complex (av 2.27 Å), while the Co−N$_{Amine}$ and Co−N$_{Py}$ distances are similar. A search of the Cambridge Crystallographic Database (version 5.30 (November)) revealed that **2-ClO$_4$** is the first structurally characterized Co(II) flavonolate complex. One Co(III) flavonolate complex has been previously characterized by X-ray crystallography.[39]

The cationic portions of the Cu(II) and Zn(II) analogues **4-ClO$_4$·Et$_2$O** and **5-ClO$_4$·2CH$_2$Cl$_2$** are shown in Figure 3. The Cu(II) center in **4-ClO$_4$·Et$_2$O** is distorted square pyramidal (τ = 0.11).[36] For the Zn(II) complex, there are two cation/anion pairs per asymmetric unit. The cations have only minor differences in bond lengths/angles involving the Zn(II) center and both exhibit a distorted square pyramidal geometry (τ = 0.35).[36] The overall features of 6-Ph$_2$TPA chelate ligand coordination in the cationic portions of **4-ClO$_4$·Et$_2$O** and **5-ClO$_4$·2CH$_2$Cl$_2$** differ in terms of the M−N$_{PhPy}$ distance, which is ~0.24 Å longer in the Cu(II) complex, and the M−N$_{Py}$ and M−N$_{Amine}$ distances which are > 0.05 Å longer in the Zn(II) complex. In both **4-ClO$_4$·Et$_2$O** and **5-ClO$_4$·2CH$_2$Cl$_2$** the coordination of the flavonolate ligand involves a shorter bonding interaction between the metal and the deprotonated hydroxyl donor (1.921(3) and 1.951(2) Å, respectively) and a longer bond with the ketone oxygen (2.010(3) and 2.1175(19) Å, respectively). Several Cu(II) complexes having a 3-Hfl ligand have been

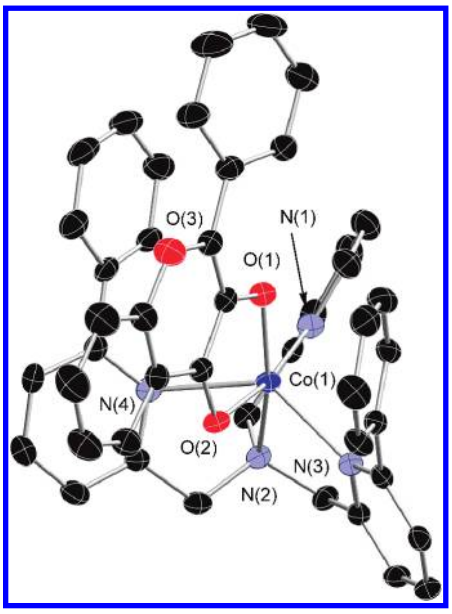

Figure 2. Thermal ellipsoid drawing (50% probability) of the cationic portion of one of the two cations present in the asymmetric unit of **2-ClO$_4$·2CH$_3$CN**. Hydrogen atoms have been omitted for clarity.

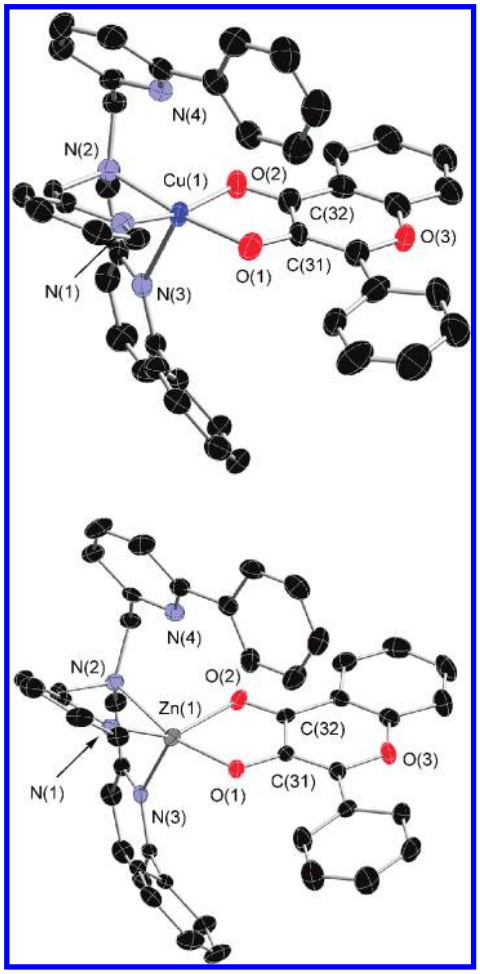

Figure 3. Thermal ellipsoid drawings (50% probability) of the cationic portions of **4-ClO$_4$·Et$_2$O** (top) and **5-ClO$_4$·2CH$_2$Cl$_2$** (bottom). Hydrogen atoms have been omitted for clarity.

previously characterized by X-ray crystallography.[40−46] A portion of these compounds have a bidentate or

(39) One Co(III) flavonolate complex supported by a salen ligand is listed in the Cambridge Crystallographic Database: Hiller, W.; Nishinaga, A.; Rieker, A. *Z. Naturforsch., B: Chem. Sci.* **1992**, *47*, 1185.
(40) Kaizer, J.; Pap, J.; Speier, G.; Parkanyi, L. *Eur. J. Inorg. Chem.* **2004**, 2253–2259.
(41) Lippai, I.; Speier, G.; Huttner, G.; Zsolnai, L. *Chem. Commun.* **1997**, 741–742.

tridentate supporting chelate ligand,[40−43] whereas others are species such as $[Cu(3\text{-Hfl})_2(py)_2]$ and $[Cu(3\text{-Hfl})_2]$. In these two types of complexes, the Cu−O bond distances are generally in the range of 1.90−2.21 Å, and the Δ_{M-O} varies from 0.04 to 0.29 Å.[47] For Zn(II), three 3-Hfl complexes, having either a bidentate or tridentate supporting chelate ligand, have been previously reported.[48−50] These complexes exhibit a range of Zn−O distances of 1.98−2.24 Å and Δ_{M-O} values of 0.16−0.26 Å. The bond lengths and Δ_{M-O} values for **4-ClO$_4$·Et$_2$O** and **5-ClO$_4$·2CH$_2$Cl$_2$** fall within the noted ranges.

Considering the entire series of 6-Ph$_2$TPA-supported complexes, the asymmetry in terms of the M−O interactions in **5-ClO$_4$·2CH$_2$Cl$_2$** ($\Delta_{M-O} \sim 0.17$ Å) is slightly less than that found in the Co(II) derivative **2-ClO$_4$** ($\Delta_{M-O} \sim 0.21$ Å), considerably greater than that found in the Mn(II) and Ni(II) analogues ($\Delta_{M-O} < 0.04$ Å), and approximately double that found in the Cu(II) complex ($\Delta_{M-O} \sim 0.09$ Å). Hence, in the series of 6-Ph$_2$TPA supported complexes, the asymmetry of flavonolate coordination increases in the order Mn (II) ~ Ni(II) < Cu(II) < Zn(II) < Co(II).

Examination of the bond lengths within the coordinated flavonolate ligands of **1−5-ClO$_4$** revealed that the Mn(II), Co(II), Ni(II), and Zn(II) complexes exhibit only a slight elongation (0.02−0.03 Å) of the C(32)−O(2) bond involving the ketone moiety, and a slight contraction (~0.04 Å) of the C(31)−O(1) bond of the hydroxyl donor, relative to the distances found in uncoordinated flavonol (1.232(3) and 1.357(3) Å, respectively).[51] The Cu(II) analogue **4-ClO$_4$·Et$_2$O** exhibits C−O distances (C(32)−O(2) 1.252(5) Å; C(31)−O(1), 1.349(5) Å) that are quite close to those of the free flavonol.[51] Notably, the Cu(II) complex exhibits a short C(31)−C(32) bond (1.399(6) Å) relative to that found in the other 6-Ph$_2$TPA-supported complexes (av 1.45 Å). A similar short C−C bond length was found in [Cu(II)(bpy)(3-Hfl)(2-HOC$_6$H$_4$COCO$_2$)] (1.369(14) Å),[41] but other known Cu(II) flavonolate derivatives exhibit a distance of ~1.44 Å.[42−46] Overall, the bond lengths within the flavonolate ligands of **1−5-ClO$_4$** are minimally affected by the identity of the metal ion present.

Spectroscopic, Magnetic, and Redox Properties of 1−5-OTf. Presented in Table 3 are selected spectroscopic features of **1−5-OTf**. Also given are magnetic moments, which indicate that each complex has a high-spin divalent metal center, and redox features identified in the range of +1.4 V to −1.0 V. ^{1}H NMR spectra were also collected for the Co(II), Ni(II), and Zn(II) complexes.

Infrared Spectroscopy. In the solid state, each complex exhibits a $\nu_{C=O}$ vibration for the coordinated flavonolate ketone moiety. The highest energy $\nu_{C=O}$ is found for the cobalt complex **2-OTf**, which is consistent with the fact that the perchlorate analogue has the longest M(1)−O(2) distance of the series of complexes and therefore should polarize the carbonyl to the weakest extent. That being said, we note that the C(32)−O(2) bond lengths throughout the series **1−5-ClO$_4$** are the same within experimental error. The Cu(II) complex **4-OTf** exhibits the lowest energy $\nu_{C=O}$ vibration, which is consistent with the structural data for **4-ClO$_4$**, which has the shortest M(1)-O(2) distance of the series of complexes.

UV−vis Spectroscopy. Neutral flavonol compounds exhibit an absorption feature in the range of 350−380 nm, which is termed band I and is assigned to the $\pi \rightarrow \pi^*$ transition.[52] When dissolved in CH$_3$CN under anaerobic conditions, each complex **1−5-OTf** exhibits an intense absorption feature in the range of 420−443 nm. For comparison, we have measured the absorption features of a flavonolate salt ([Me$_4$N$^+$][3Hfl$^-$]) in CH$_3$CN (band I, λ_{max} = 458 nm).[53] For each metal complex, a hypsochromic shift of the absorption band is found relative to the 3-Hfl salt, with the exact shift being influenced by the nature of the metal ion. For example, the Mn(II) complex **1-OTf** exhibits band I at 431 nm. This matches well with the band I reported for Mn(3-Hfl)$_2$-(py)$_2$ (432 nm).[23] To our knowledge, absorption spectra of an enzyme/substrate complex a Mn(II)-containing quercetinase enzyme have not been reported.[11] Notably, the Ni(II) complex **3-OTf** exhibits the smallest shift with band I at 443 nm, and the zinc and cobalt complexes **5-OTf** and **2-OTf** exhibit the largest shifts, with band I at 420 and 422 nm, respectively. For the Ni(II)-containing form of QueD from *Streptomyces* sp. FLA, under anaerobic conditions, addition of quercetin at pH = 8 produces an absorption feature at 385 nm, which represents a hypsochromic shift relative to the absorption feature of free quercetin at pH = 8 (λ_{max} = 391 nm). Similarly, addition of quercetin to anaerobic cobalt-containing QueD produces a band I absorption at 378 nm.[12] Thus, in both the synthetic and enzyme systems, the presence of Co(II) produces a more significant hypsochromic shift in band I. The absorption maximum found for the Cu(II) complex **4-OTf** (428 nm) is within the reported range for Cu(II) flavonolate complexes (416−434 nm).[19] The band I absorption of [Zn(3-Hfl)(idpa)]ClO$_4$ (idpa = 3,3′-iminobis(*N*,*N*-dimethylpropylamine) has been reported as 419 nm, which matches well with that found for **5-ClO$_4$**.[54] Overall, from the limited set of well-characterized divalent metal 3-Hfl complexes reported in the literature to date (including those reported herein), the hypsochromic shift of the band I $\pi \rightarrow \pi^*$ transition

(42) Balogh-Hergovich; Kaizer, J.; Speier, G.; Huttner, G.; Zsolnai, L. *Inorg. Chim. Acta* **2000**, *304*, 72–77.
(43) Balogh-Hergovich, E.; Kaizer, J.; Speier, G.; Huttner, G.; Jacobi, A. *Inorg. Chem.* **2000**, *39*, 4224–4229.
(44) Okabe, N.; Yamamoto, E.; Yasunori, M. *Acta Crystallogr., Sect. E: Struct. Rep. Online* **2003**, *59*, m715–m716.
(45) Balogh-Hergovich, E.; Speier, G.; Argay, G. *J. Chem. Soc., Chem. Commun.* **1991**, 551–552.
(46) Balogh-Hergovich, E.; Kaizer, J.; Speier, G.; Argay, G.; Párkányi, L. *J. Chem. Soc., Dalton Trans.* **1999**, 3847–3854.
(47) The Cu(II) complex [Cu(II)(bpy)(fla)(2-HOC$_6$H$_4$COCO$_2$)] has been reported to have Cu−O bond lengths of 2.190(9) and 1.760(11) Å and Δ_{M-O} = 0.43 Å.[41]
(48) Balogh-Hergovich, E.; Kaizer, J.; Speier, G.; Huttner, G.; Rutsch, P. *Acta Crystallogr., Sect. C: Cryst. Struct. Commun.* **1999**, *55*, 557–558.
(49) Annan, T. A.; Peppe, C.; Tuck, D. G. *Can. J. Chem.* **1990**, *68*, 423–430.
(50) Kaizer, J.; Kupán, A.; Pap, J.; Speier, G.; Réglier, M.; Michel, G. *Z. Kristallogr. -New Cryst. Struct.* **2000**, *215*, 571–572.
(51) Etter, M. C.; Urbanczyk-Lipkowska, Z.; Baer, S.; Barbara, P. F. *J. Mol. Struct.* **1986**, *144*, 155–167.
(52) Jurd, L.; Geissman, T. A. *J. Org. Chem.* **1956**, *21*, 1395–1401.
(53) Barhács, et al. report the absorption maxium of [K][3-Hfl] to be 465 nm. Barhács, L.; Kaizer, J.; Speier, G. *J. Org. Chem.* **2000**, *65*, 3449−3452.
(54) Barhács, L.; Kaizer, J.; Speier, G. *J. Mol. Catal. A* **2001**, *172*, 117–125.

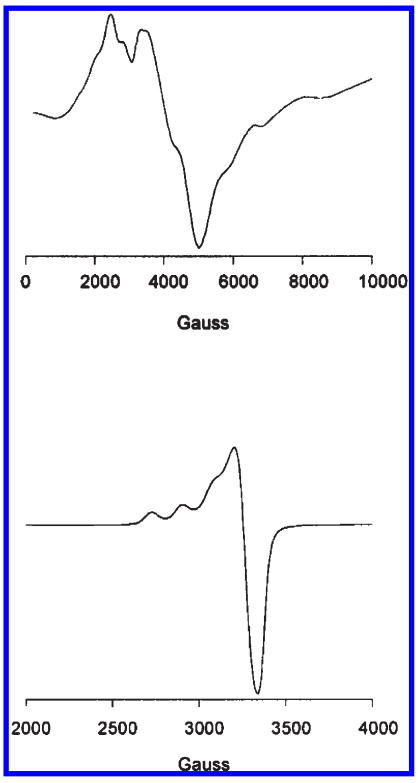

Figure 4. EPR spectra of **1-OTf** and **4-OTf**. Spectra were recorded at 4.7 K, 1.002 mW microwave power, and 9.39 GHz. The samples were ≤1 mM in CH_3CN.

(relative to the free 3-Hfl anion) generally increases in the order Ni(II) < Mn(II) < Cu(II) < Zn(II), Co(II).

EPR Spectroscopy. EPR spectra were obtained for the Mn(II) and Cu(II) complexes of the series (**1-OTf** and **4-OTf**) and are shown in Figure 4. The spectrum collected for **1-OTf** is similar to the spectrum collected for the hydroxamate-bridged dimanganese complex $[(6\text{-}Ph_2\text{-}TPAMn)(\mu\text{-}ONHC(O)CH_3)_2](ClO_4)_2$.[25] No hyperfine coupling is discernible in the spectrum of either the **1-OTf** or the Mn(II) hydroxamate complex. The similarity of these spectra suggested to us the possible formation of a flavonolate-bridged dimanganese complex in solution. Reactivity studies outlined below provide additional evidence for the chemical similarities of **1-OTf** and the hydroxamate complex in CH_3CN. We note that the Mn(II)-containing form of the *B. subtilis* quercetin dioxygenase in the presence of quercetin under anaerobic conditions exhibits a six-line EPR signal at $g = 2$, with a hyperfine coupling constant of approximately 93 G.[11] A second, less intense six-line signal is also present at $g = 9$ and exhibits a similar hypefine coupling constant. This data is consistent with the enzyme containing a mononuclear pseudo-octahedral Mn(II) center having oxygen/nitrogen ligands.[55]

The axial EPR spectrum of **4-OTf** is consistent with the distorted square pyramidal geometry of the Cu(II) center and a $d_{x^2-y^2}$ ground state ($g_\parallel \sim 2.24$; $g_\perp \sim 2.06$; $A_\parallel \sim 180$ G). The anaerobic enzyme/substrate complex of the quercetinase enzyme from *A. japonius* exhibits an EPR signal with $g_\parallel = 2.366$ and $A_\parallel \sim 110$ G.[56]

(55) Reed, G. H.; Markham, G. D. *Biological Magnetic Resonance*; Berliner, L. J., Rueben, J., Eds.; Plenum: New York, 1978; Vol. *6*, pp 73−142.
(56) Spectrum obtained at 77 K.

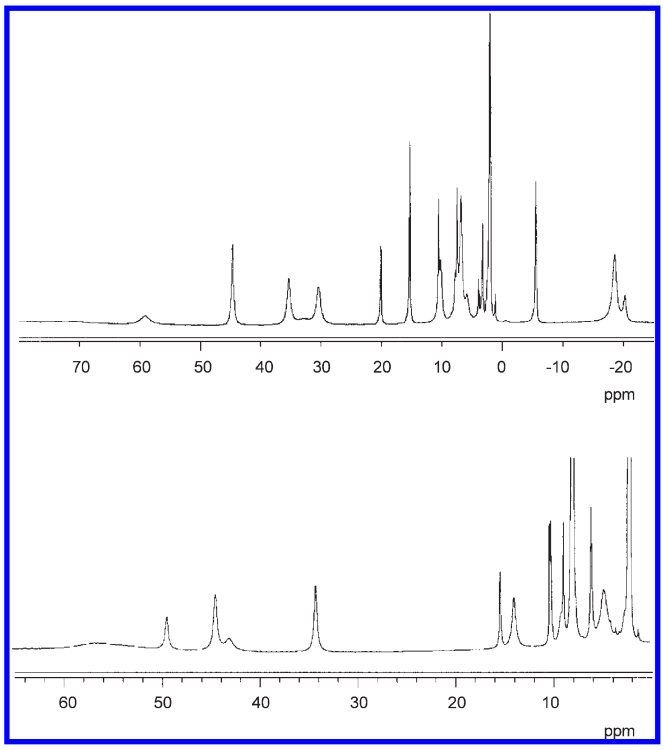

Figure 5. ^1H NMR spectra of **2-OTf** (top) and **3-OTf** (bottom) in CD_3CN at ambient temperature.

^1H NMR Spectroscopy. The ^1H NMR spectra of analytically pure **2-OTf**, **3-OTf**, and **5-OTf** were measured in CD_3CN at ambient temperature. The spectra for the paramagnetic Co(II) and Ni(II) complexes are shown in Figure 5. While full assignment of the resonances of **2-OTf** and **3-OTf** have not been made, the spectra are clearly distinct from those of other complexes of bidentate ligands (e.g., hydroxamate derivatives) and can be used to evaluate complex purity and reactivity.[25] There are no concentration dependent changes in these NMR spectra. Attempts were made to collect two-dimensional COSY spectra to assign the pyridyl ring proton resonances of the 6-Ph_2TPA ligands in **2-OTf** and **3-OTf**.[26] Unfortunately these experiments did not reveal any crosspeaks. It is important to note that the total number of paramagnetically shifted resonances in the spectra of **2-OTf** and **3-OTf** is consistent with the presence of an effective plane of symmetry containing the pyridyl donor, which gives equivalent phenyl-appended pyridyl donors. This indicates that the solution structure of these compounds is generally similar to that found in the solid state. The features of the ^1H and ^{13}C NMR spectra of **5-OTf** (see Experimental Section) are consistent the formation of a six-coordinate Zn(II) center in solution via coordination of all donors of the supporting 6-Ph_2TPA ligand. Most notably, the total number of carbon signals is consistent with the presence of an effective plane of symmetry that makes the phenyl-appended pyridyl donors equivalent.

Cyclic Voltammetry. The redox properties of **1**−**5-OTf** were examined by cyclic voltammetry. An irreversible oxidation wave was identified for **1-OTf** and **3**−**5-OTf**, and the Ep_a values are given in Table 3. The Co(II) complex **2-OTf** did not show any electrochemical behavior in the range examined. A quasi-reversible reduction peak at −1088 mV versus Fc/Fc^+ (Supporting Information, Figure S1) for

4-OTf has been tentatively assigned to the Cu(II)/Cu(I) couple, as no other compound of the group has waves at potentials lower than Fc/Fc^+. These data for **1**−**5-OTf** indicate that the nature of the divalent metal influences the redox potential of the coordinated flavonolate over a range of ~300 mV. The differences in oxidation potential found for this series of complexes depend on the metal and/or the solution structure of the metal complex. The Mn(II) derivative **1-OTf**, which based on EPR, may form binuclear species in solution, has the lowest potential, indicating that the flavonolate is a better reductant toward O_2 than the same ligand in the Ni(II), Cu(II), and Zn(II) analogue complexes. For the Ni(II) and Zn(II) complexes **3-ClO$_4$** and **5-ClO$_4$**, irreversible oxidation of the flavonolate ligand occurs at +0.506 and +0.536 V versus Fc/Fc^+, respectively. For the Cu(II) complex, which is distorted square pyramidal in acetonitrile, the potential is more positive (+0.660 V). Potentials previously reported for 3-Hfl complexes of the general formula $[M(3\text{-Hfl})(H_2O)_n]Cl$ (M = Cu, n = 2; M = Fe, n = 4) are in the same range as those reported herein.[57]

Ligand Exchange Reactivity. The results of initial electrospray ionization mass spectrometry experiments suggested that the Mn(II) flavonolate complex **1-OTf** would undergo reaction with available Zn(II) ion to produce a ligand exchange product, $[(6\text{-Ph}_2\text{TPA})Zn(OTf)]^+$. To examine this reactivity, in independent NMR tube experiments, $[(6\text{-Ph}_2\text{TPA})Mn(3\text{-Hfl})]OTf$ was treated with an equimolar amount of $M(ClO_4)_2\cdot 6H_2O$ (M = Co(II), Ni(II), and Zn(II)) in CD_3CN. For each reaction, well resolved ^1H NMR spectra consistent with the quantitative formation of a divalent metal solvate complex of the added metal, $[(6\text{-Ph}_2\text{TPA})M(CD_3CN)_n](X)_2$ (n = 1 or 2; X = OTf^- or ClO_4^-) were obtained.[25,26] A yellow-green precipitate formed in each reaction mixture and was identified as $[Mn(3\text{-Hfl})_2\cdot 0.5H_2O]$ by elemental analysis. This compound was isolated from the reaction mixture involving Ni(II) by selective crystallization in 39% yield (for 0.5 equiv). In addition to the stoichiometric formation of $[(6\text{-Ph}_2\text{TPA})M(CD_3CN)_n](X)_2$ and 0.5 equiv of $[Mn(3\text{-Hfl})_2\cdot 0.5H_2O]$, mass balance requires the formation of 0.5 equiv of MnX_2 salt (eq 1), which could not be isolated from the reaction mixture. Notably, we found that the Mn(II) hydroxamate complex $[(6\text{-Ph}_2\text{TPAMn})(\mu\text{-ONHC(O)CH}_3)_2](ClO_4)_2$[25] also reacts with $M(ClO_4)_2\cdot 6H_2O$ to produce $[(6\text{-Ph}_2\text{TPA})M(CD_3CN)](X)_2$ (M = Co, Ni, Zn; X = OTf^- or ClO_4^-; eq 2), as determined by ^1H NMR. The similarity in EPR spectral features (vida supra) and reactivity of $[(6\text{-Ph}_2\text{TPA})Mn(3\text{-Hfl})]OTf$ and $[(6\text{-Ph}_2\text{TPAMn})(\mu\text{-ONHC(O)CH}_3)_2](ClO_4)_2$ suggest that

$$\text{M} = \text{Co, Ni, Zn; X} = \text{OTf}^- \text{or } \text{ClO}_4^-$$

$$[(6\text{-Ph}_2\text{TPA})Mn(3\text{-Hfl})]OTf + M(ClO_4)_2\cdot 6H_2O + nCD_3CN \rightarrow [(6\text{-Ph}_2\text{TPA})M(CD_3CN)_n](X)_2 + 0.5MnX_2 + 0.5[Mn(3\text{-Hfl})_2\cdot 0.5H_2O] + 5.75H_2O \quad (1)$$

$$[(6\text{-Ph}_2\text{TPA})Mn(ONHC(O)CH_3)]ClO_4 + M(ClO_4)_2\cdot 6H_2O + nCD_3CN \rightarrow [(6\text{-Ph}_2\text{TPA})M(CD_3CN)_n](X)_2 + 0.5MnX_2 + 0.5[Mn(ONHC(O)CH_3)_2] + 6H_2O \quad (2)$$

(57) de Souza, R. F. V.; Sussuchi, E. M.; De Giovani, W. F. *Synth. React. Inorg. Met.-Org. Chem.* **2003**, *33*, 1125–1144.

the compounds may have similar solution structures. We propose that these structures include μ-η^1:η^2-coordination of the chelate anion (3-Hfl or acetohydroxamate) as is found in the X-ray structure of $[(6\text{-Ph}_2\text{TPAMn})(\mu\text{-ONHC(O)CH}_3)_2](ClO_4)_2$.[25] In this coordination motif, each Mn(II) center coordinates the anionic oxygen of each bridging ligand. We propose that from this structure an equilibrium mixture is formed, and is composed of 0.5 equiv of $[Mn(3\text{-Hfl})_2\cdot 0.5H_2O]$, 0.5 equiv of free chelate ligand, and 0.5 equiv of $[(6\text{-Ph}_2\text{TPA})Mn(CD_3CN)_2](X)_2$ (Scheme 3). Formation of the final product mixture, including 1 equiv of $[(6\text{-Ph}_2\text{TPA})M(CD_3CN)_n](X)_2$ (M = Co, Ni, Zn), could result from coordination of the free divalent metal ion to the free chelate ligand, and displacement of Mn(II) (as MnX_2) from $[(6\text{-Ph}_2\text{TPA})Mn(CD_3CN)_2](X)_2$. The latter reaction has been independently investigated by ^1H NMR and found to occur rapidly in CD_3CN for M = Co(II), Ni(II), and Zn(II).

In another type of ligand exchange reaction, we found that treatment of the non-manganese flavonolate complexes $[(6\text{-Ph}_2\text{TPA})M(3\text{-Hfl})]OTf$ (M = Co (**2-OTf**), Ni (**3-OTf**), and Cu (**4-OTf**)) with 0.5 equiv of $Zn(ClO_4)_2\cdot 6H_2O$ in CD_3CN results in the formation of $[(6\text{-Ph}_2\text{TPA})M(CD_3CN)_n](X)_2$ (n = 1 or 2; X = OTf^- or ClO_4^-) species as indicated by ^1H NMR. Hence, in these reactions flavonolate ligand exchange occurs, but no change in the metal bound by the 6-Ph$_2$TPA ligand takes place. The other product in the reaction is $[Zn(3\text{-Hfl})_2\cdot 2H_2O]$ (eq 3), which is a poorly soluble yellow precipitate. This material was identified by independent synthesis and characterization, followed by comparison of UV−vis and ^1H NMR properties between the reaction product and the independently generated material.

$$\text{M} = \text{Co, Ni, Cu; X} = \text{OTf}^- \text{or } \text{ClO}_4^-$$

$$[(6\text{-Ph}_2\text{TPA})M(3\text{-Hfl})]OTf + 0.5Zn(ClO_4)_2\cdot 6H_2O + nCD_3CN \rightarrow [(6\text{-Ph}_2\text{TPA})M(CD_3CN)_n](X)_2 + 0.5[Zn(3\text{-Hfl})_2\cdot 2H_2O] + 2H_2O \quad (3)$$

What about Fe(II)? The quercetinase enzyme from *B. subtilis* was originally described as a non-heme iron enzyme.[10] However, the turnover number for this enzyme was reported to be 2 orders of magnitude lower than for the Cu(II)-containing *A. flavus*, which led researchers to suggest that Fe(II) might not be the correct cofactor for the enzyme. Follow-up studies suggested that Mn(II) was probably the correct cofactor for the *B. subtilis* enzyme.[11] To date, only two iron flavonolate complexes, both Fe(III) derivatives, have been crystallographically characterized.[23,24]

To gauge the chemistry of Fe(II) relative to the other 3d metal ions investigated herein, we initiated attempts to prepare a Fe(II) flavonolate complex supported by the 6-Ph$_2$TPA ligand. In our first approach, treatment of 6-Ph$_2$TPA with equimolar amounts of $Fe(ClO_4)_2\cdot 6H_2O$, 3-hydroxyflavonol, and $Me_4NOH\cdot 5H_2O$ under a N_2 atmosphere, followed by stirring overnight, workup, and crystallization from CH_3CN/Et_2O resulted in the deposition of dark brown single crystals. X-ray crystallographic analysis of these crystals revealed the formation of the diiron(III) μ-oxo compound $[(6\text{-Ph}_2\text{TPAFe}(3\text{-Hfl}))_2(\mu\text{-O})](ClO_4)_2$

Scheme 3. Proposed Reaction Pathway for Ligand Exchange in the Reaction of **1-OTf** with Divalent Metal Perchlorate Salts

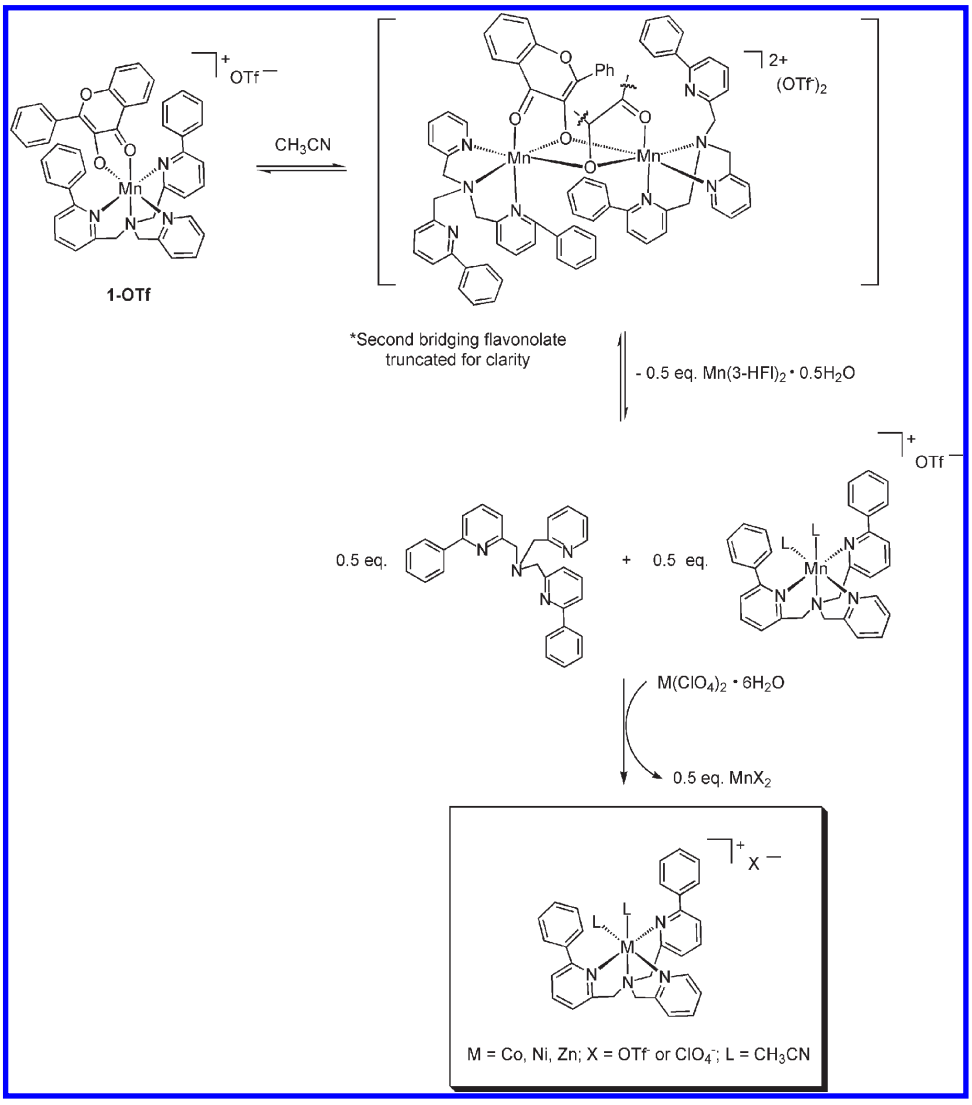

(**6**·**2.5CH$_3$CN**, Figure 7). The structural and spectroscopic properties of this complex are discussed in detail below. However, as an approach toward understanding the reaction pathway leading to the formation of **6**, we further explored the synthetic conditions. Treatment of 6-Ph$_2$TPA with Fe(ClO$_4$)$_2$·6H$_2$O in CH$_3$CN, followed by recrystallization from CH$_3$CN/Et$_2$O, yielded [(6-Ph$_2$TPA)Fe(CH$_3$CN)](ClO$_4$)$_2$ (**7**) as pale yellow crystals. Characterization details for this Fe(II) complex are given in the Supporting Information. Treatment of **7** with equimolar amounts of 3-hydroxyflavonol and Me$_4$NOH·5H$_2$O in methanol, and stirring for 15 min under a freshly purged N$_2$ atmosphere, gave a green-yellow solution from which, after workup, a green-yellow precipitate was isolated. The analytical and spectroscopic properties of this complex are consistent with the formulation [(6-Ph$_2$TPA)Fe(3-Hfl)]ClO$_4$ (**8**). For this complex, the flavonolate $\nu_{C=O}$ vibration is at 1558 cm^{-1}, and the band I $\pi \rightarrow \pi^*$ transition is at 415 nm ($\varepsilon \sim 14700$ M^{-1} cm^{-1}). These features are similar to those found for the Co(II) derivative **2-OTf**, suggesting that the flavonolate ligand may be coordinated with a Δ_{M-O} similar to that found in the cobalt complex. The magnetic moment for **8** ($\mu_{eff} = 4.7\ \mu_B$) is consistent with the presence of a high-spin Fe(II) center.[58] The ^{1}H NMR spectrum of **8** contains several paramagnetically shifted resonances over a range of ~110 ppm (Figure 6). Investigation of the redox properties of **8** by cyclic voltammetry (CH_2Cl_2, [**8**] = 1 mM, Bu_4NClO_4 (0.1 M) supporting electrolyte, scan rate 50−100 mV/s) revealed a quasi-reversible couple at ~−0.05 V versus ferrocene/ferrocenium, which is assigned as the Fe(II)/Fe(III) couple. No redox activity was found at more positive potentials, indicating that upon oxidation of the iron center, the redox potential for the coordinated flavonolate is shifted from that observed for the other divalent metal 3-Hfl complexes. This redox behavior is consistent with the observed metal-centered O$_2$ reactivity described below.

Complex **8** is very air sensitive, which complicated our efforts to characterize it, especially in solution. Exposure of a CH$_3$CN solution of **8** to air results in a rapid darkening of the color, which corresponds to the formation of the μ-oxo compound **6**. This complex was characterized by X-ray crystallography, elemental analysis,

(58) Huheey, J. E.; Keiter, E. A.; Keiter, R. L. *Inorganic Chemistry: Principles of Structure and Reactivity*; Harper Collins: New York, 1993.

Scheme 4

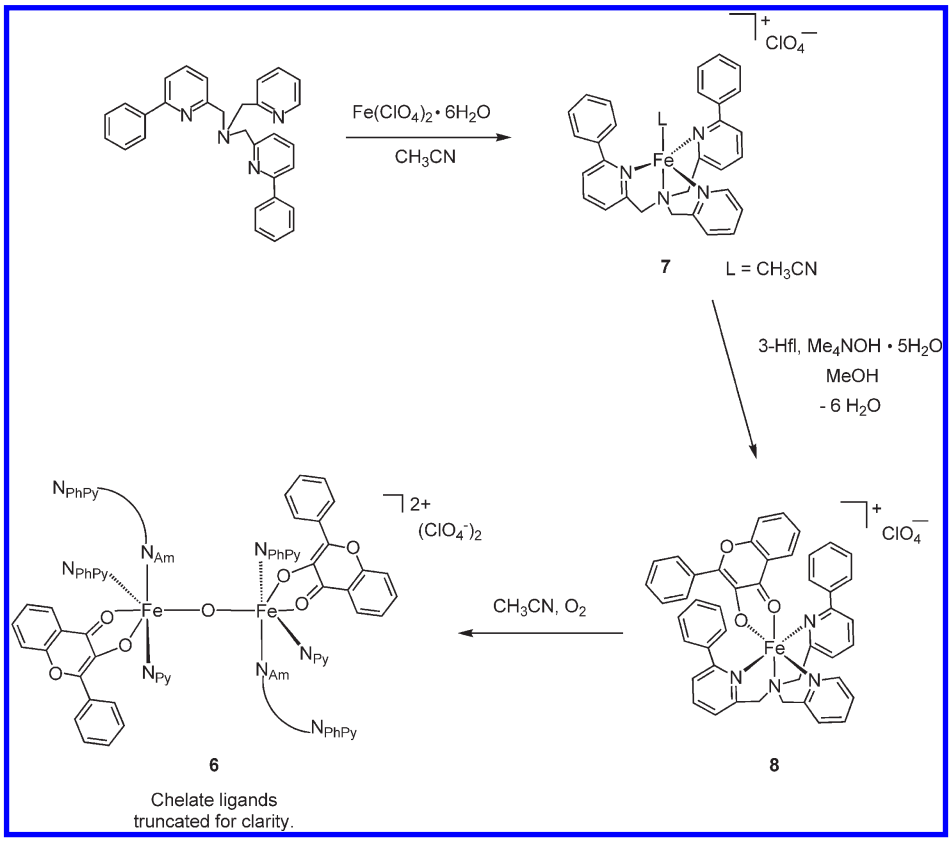

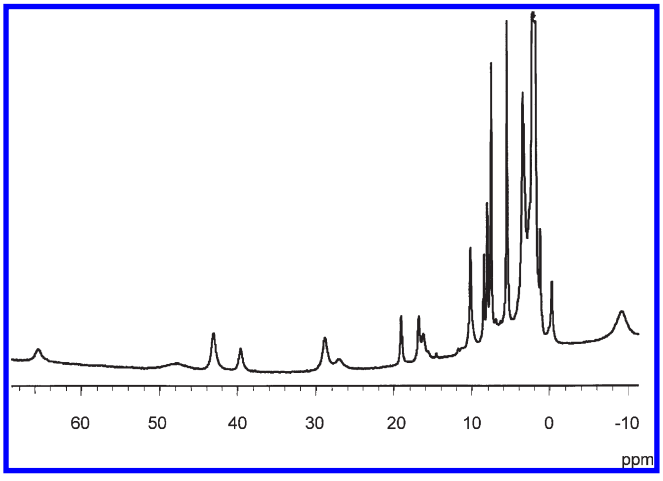

Figure 6. ^{1}H NMR spectrum of [(6-Ph$_2$TPA)Fe(3-Hfl)]ClO$_4$ (**8**) in CD$_3$CN at ambient temperature. In addition to the resonances shown, broad peaks are also present at 112 and 92 ppm.

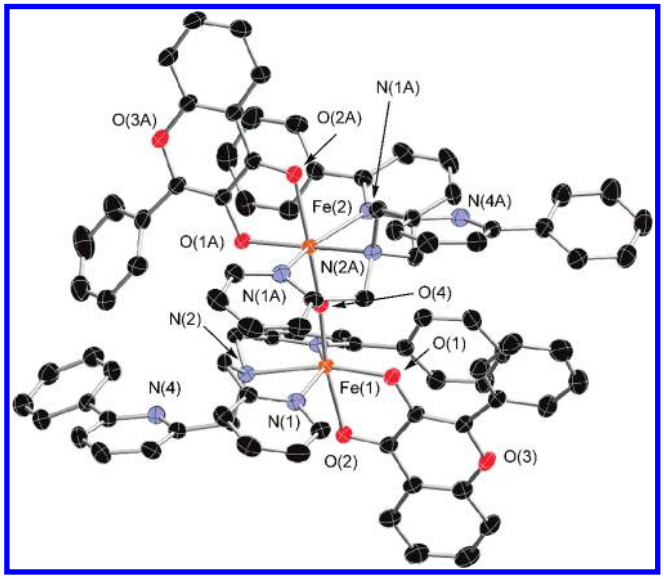

Figure 7. Thermal ellipsoid drawings (50% probability) of the cationic portions of **6·2.5CH$_3$CN**. Hydrogen atoms have been omitted for clarity.

UV−vis, FTIR, and mass spectrometry. A summary of the iron coordination chemistry is shown in Scheme 4.

The cationic portion of **6·2.5CH$_3$CN** is shown in Figure 7. Details of the X-ray data collection of this complex are given in Table 4. Selected bond distances and angles are given in Table 5 and Supporting Information, Table S2, respectively. Each Fe(III) center has a κ^3-6-Ph$_2$TPA ligand, a bidentate flavonolate ligand, and the μ-oxo bridge. The flavonolate ligands are coordinated to Fe(1) and Fe(2) with Δ_{M-O} = 0.17 and 0.14 Å, respectively. This is similar to the coordination found in the Co(II) and Zn(II) flavonolate complexes **2-ClO$_4$** and **5-ClO$_4$·CH$_2$Cl$_2$**. Similarly, the Fe(III) complexes [(salen)-Fe(III)(3-Hfl)] and [Fe(4′-MeOflaH)$_3$] have Δ_{M-O} = 0.18 and 0.15 Å, respectively.[23,24] Thus, all of the Fe(III) flavonolate complexes that have been structurally characterized to date exhibit very similar levels of asymmetry with respect to flavonolate coordination. The Fe−O(flavonolate) bond distances are also very similar in all three compounds. We note that the flavonolate ketone oxygen donor is positioned *trans* to the μ-oxo bridge in **6·2.5CH$_3$CN**, whereas the deprotonated oxygen donor is

Table 4. Summary of X-ray Data Collection and Refinement for **6·2.5CH$_3$CN**[a]

empirical formula	$C_{95}H_{77.5}Cl_2Fe_2N_{10.5}O_{15}$
M_r	1788.78
crystal system	triclinic
space group	$P\bar{1}$
a/ Å	14.02370(10)
b/ Å	15.2054(2)
c/ Å	21.6638(3)
α/ deg	70.1168(7)
β/ deg	74.8473(7)
γ/ deg	81.5826(8)
V/ Å^3	4184.67(9)
Z	2
D_c/Mg m^{-3}	1.420
T/ K	150(1)
color	red
crystal habit	prism
crystal size/ mm	0.28 × 0.18 × 0.15
diffractometer	Nonius KappaCCD
μ/ (mm^{-1})	0.486
$2\theta_{max}$/ deg	54.92
completeness to θ (%)	99.0
reflections collected	35639
independent reflections	18968
R_{int}	0.0393
variable parameters	1151
$R1/wR2$[b]	0.0460/0.1010
goodness-of-fit (F^2)	1.019
$\Delta\rho_{max/min}$/e Å^{-3}	0.397/−0.487

[a] Radiation used: Mo Kα (λ = 0.71073 Å). [b] $R1 = \sum||F_o| - |F_c||/\sum|F_o|$; $wR2 = [\sum w(F_o^2 - F_c^2)^2/\sum w(F_o^2)^2]^{1/2}$, where $w = 1/[\sigma^2(F_o^2) + (aP)^2 + bP]$.

Table 5. Selected Bond Distances (Å) for **6·2.5CH$_3$CN**

Fe(1)−O(1)	1.9712(14)	Fe(2)−O(1A)	1.9655(14)
Fe(1)−O(2)	2.1460(15)	Fe(2)−O(2A)	2.1054(15)
Fe(1)−O(4)	1.7890(14)	Fe(2)−O(4)	1.7992(14)
Fe(1)−N(1)	2.1679(17)	Fe(2)−N(1A)	2.1822(18)
Fe(1)−N(2)	2.2489(17)	Fe(2)−N(2A)	2.2180(18)
Fe(1)−N(3)	2.2241(17)	Fe(2)−N(3A)	2.2109(18)
O(1)−C(31)	1.330(3)	O(1A)−C(31A)	1.326(3)
O(2)−C(32)	1.271(3)	O(2A)−C(32A)	1.274(2)

trans to the tertiary amine nitrogen. This results in a meridional donor array from the κ^3-bound chelate ligand. The Fe−O bond distances involving the oxo bridge in **6·2.5CH$_3$CN** are within experimental error identical to those found in [(6-C$_6$H$_4$O-TPAFe)$_2$(μ-O)](BPh$_4$)$_2$.[59] The average Fe−N distance in **6·2.5CH$_3$CN** (∼2.20 Å) is slightly longer than what is found in [(6-C$_6$H$_4$-TPAFe)$_2$-(μ-O)](BPh$_4$)$_2$ (∼2.18 Å). However, both distances are consistent with a high-spin (S = 5/2) state for each iron center.[60]

A vibration at 1549 cm^{-1} in the solid state infrared spectrum of **6** is assigned as the $\nu_{C=O}$ vibration of the flavonolate, based on comparison to the spectral features of [(salen)Fe(III)(3-Hfl)] (1549 cm^{-1}).[24] Compound **6** is slightly soluble in methanol and exhibits absorption bands at 388 and 490 nm. Unlike its Fe(II) flavonolate precursor **8**, an absorption feature for the flavonolate ligand in the region of 400−450 nm could not be readily identified. The absorption features of **6** and **8** are compared in Figure 8. For [(salen)Fe(III)(3-Hfl)], an absorption maximum at 407 nm was reported.[24] The ^{1}H NMR spectrum of **6** in d_4-methanol consists of broad resonances in the range of 0 to ∼40 ppm (Supporting Information, Figure S3). Several features of this spectrum are significantly overlapped in the aromatic range (−10 to 40 ppm), consistent with the presence of several types of aryl protons. The dramatically different features of this spectrum versus that found for [(6-Ph$_2$TPA)Fe(3-Hfl)]ClO$_4$ (**8**, Figure 6) is likely due to antiferromagnetic coupling of the S = 5/2 metal centers via the oxo bridge.[59,61,62]

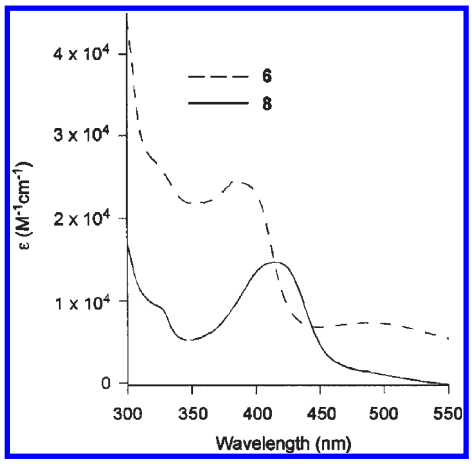

Figure 8. UV−vis absorption features of [(6-Ph$_2$TPAFe(3-Hfl))$_2$(μ-O)](ClO$_4$)$_2$ (**6**) and [(6-Ph$_2$TPA)Fe(3-Hfl)]ClO$_4$ (**8**).

Final Comments

The chemistry of metal complexes of flavonolate ligands is of significant current interest. Metal flavonolate complexes have been prepared and investigated for their antioxidant and DNA cleavage reactivity.[63−74] Because of their biological relevance, metal flavonolate complexes have also been the subject of several recent computational investigations.[75−78] As noted in the introduction, fungal and bacterial quercetinase enzymes have been shown to exhibit varying levels of activity as a function of the divalent metal ion present. While

(59) Jensen, M. P.; Lange, S. J.; Mehn, M. P.; Que, E. L.; Que, L., Jr. *J. Am. Chem. Soc.* **2003**, *125*, 2113–2128.
(60) Zang, Y.; Kim, J.; Dong, Y.; Wilkinson, E. C.; Appelman, E. H.; Que, L., Jr. *J. Am. Chem. Soc.* **1997**, *119*, 4197–4205.
(61) Wu, F.-J.; Kurtz, D. M., Jr. *J. Am. Chem. Soc.* **1989**, *111*, 6563–6572.
(62) Norman, R. E.; Yan, S.; Que, L., Jr.; Backes, G.; Ling, J.; Sanders-Loehr, J.; Zhang, J. H.; O'Connor, C. J. *J. Am. Chem. Soc.* **1990**, *112*, 1554–1562.
(63) Ryan, P.; Hynes, M. J. *J. Inorg. Biochem.* **2008**, *102*, 127–136.
(64) Kazazic, S. P.; Butkovic, V.; Srzic, D.; Klasinc, L. *J. Agric. Food Chem.* **2006**, *54*, 8391–8396.
(65) de Souza, R. F. V.; De Giovani, W. F. *Spectrochim Acta A* **2005**, *61*, 1985–1990.
(66) Bukhari, S. B.; Memon, S.; Mahroof-Tahir, M.; Bhanger, M. I. *Spectrochim. Acta A* **2009**, *71*, 1901–1906.
(67) Guo, M.; Perez, C.; Wei, Y.; Rapoza, E.; Su, G.; Bou-Abdallah, F.; Chasteen, N. D. *Dalton Trans.* **2007**, 4951–4961.
(68) El Hajji, H.; Nkhili, E.; Tomao, V.; Dangles, O. *Free Radical Res.* **2006**, *40*, 303–320.
(69) de Souza, R. F. V.; De Giovani, W. F. *Redox Rep.* **2004**, *9*, 97–104.
(70) Mira, L.; Fernandez, M. T.; Santos, M.; Rocha, R.; Florencio, M. H.; Jennings, K. R. *Free Radical Res.* **2002**, *36*, 1199–1208.
(71) Tan, J.; Wang, B.; Zhu, L. *J. Biol. Inorg. Chem.* **2009**, *14*, 727–739.
(72) Tan, J.; Wang, B.; Zhu, L. *Bioorg. Med. Chem.* **2009**, *17*, 614–620.
(73) Tan, J.; Zhu, L.; Wang, B. *Dalton Trans.* **2009**, 4722–4728.
(74) El Amrani, F. B. A.; Perrelló, L.; Real, J. A.; Gozález-Álvarez, M.; Alzuet, G.; Borrás, J.; Garcia-Granda, S.; Montejo-Bernardo, J. *J. Inorg. Biochem.* **2006**, *100*, 1208–1218.
(75) Lekka, C. E.; Ren, J.; Meng, S.; Kaxiras, E. *J. Phys. Chem. B* **2009**, *113*, 6478–6483.
(76) Ren, J.; Meng, S.; Lekka, C. E.; Kaxiras, E. *J. Phys. Chem. B* **2008**, *112*, 1845–1850.
(77) Leopoldini, M.; Russo, N.; Chiodo, S.; Toscano, M. *J. Agric. Food Chem.* **2006**, *54*, 6343–6351.
(78) Cornard, J. P.; Dangleterre, L.; Lapouge, C. *Chem. Phys. Lett.* **2006**, *419*, 304–308.

a few initial investigations directed at evaluating the effect of the metal ion on flavonolate/O_2 chemistry of relevance to quercetin dioxygenase enzymes have been reported,[23,24] these studies lack a systematic approach. Specifically, the studies reported to date have included comparisons between complexes having different supporting chelate ligands and/or metal oxidation states. The research described herein is the first detailed systematic mapping of how metal ion content influences the structural, spectroscopic, redox properties, and ligand exchange reactivity of structurally related flavonolate complexes. These complexes are relevant to the metal/flavonolate adducts proposed to form in quercetinase enzymes of varying metal ion content. The results presented herein lay the groundwork for detailed O_2 reactivity studies as a function of the divalent metal ion present. These investigations are currently in progress.

Acknowledgment. The authors thank the National Science Foundation (CHE-0848858 (L.M.B.), CHE-0615479 (J.A.H.)) for financial support of this research. We also thank Ewa Szajna-Fuller for producing the X-ray crystals of [(6-Ph_2TPA)Fe(CH_3CN)]ClO_4 (**7**).

Supporting Information Available: Tables of bond angles for **1**−**5-ClO$_4$** and **6·2.5CH$_3$CN**; cyclic voltammogram for **4-OTf**; synthetic and characterization details for [(6-Ph_2TPA)Fe($NCCH_3$)]$(ClO_4)_2$ (**7**); room temperature ^{1}H NMR spectrum of **6** in CD_3OD. This material is available free of charge via the Internet at http://pubs.acs.org.